Corrosion Science 173 (2020) 108780

Contents lists available at ScienceDirect

Corrosion Science

journal homepage: www.elsevier.com/locate/corsci

The effect of time evolution and timing of the electrochemical data recording of corrosion inhibitor protection of hot-dip galvanized steel

M. Meeusen[a,*], L. Zardet[b], A.M. Homborg[c], M. Lekka[b], F. Andreatta[b], L. Fedrizzi[b], B. Boelen[d], J.M.C Mol[a], H. Terryn[a,e]

[a] Department of Materials Science and Engineering, Delft University of Technology, 2628 CD Delft, the Netherlands
[b] University of Udine, Polytechnic Department of Engineering and Architecture, Udine, Italy
[c] Netherlands Defence Academy, Het Nieuwe Diep 8, 1781 AC Den Helder, the Netherlands
[d] Tata Steel IJmuiden B.V., Research and Development, Surface Engineering – Coating Development, Ijmuiden, the Netherlands
[e] Research Group of Electrochemical an Surface Engineering (SURF), Vrije Universiteit Brussel, 1050 Brussels, Belgium

ARTICLE INFO

Keywords:
ORP-EIS
Electrochemistry
Methodology
Corrosion inhibitor

ABSTRACT

In previous work, the importance of taking the time-domain into account when studying corrosion inhibitor-containing electrochemical systems was highlighted. In this work, odd random phase electrochemical impedance spectroscopy (ORP-EIS) is applied as the electrochemical tool to study the time-effect by the evaluation of the non-stationarities per frequency decade over time for the screening of different silica- and phosphate- based corrosion inhibitors for hot-dip galvanized steel and possible corrosion inhibitor synergism. This serves as the basis for the interpretation of the results obtained from different macroscopic electrochemical techniques such as potentiodynamic polarization (PP), open circuit potential (OCP) with superimposed linear polarization resistance (LPR), electrochemical impedance spectroscopy (EIS) and electrochemical noise (EN) measurements. The analysis of the time-domain shows that all systems have a system-specific 'stabilization' time which affects the interpretation of the results obtained from the macroscopic electrochemical techniques. Furthermore, these results indicate that all corrosion inhibitors tested exhibit corrosion protective action and that the combination of both silica-based corrosion inhibitors show synergistic action on hot-dip galvanized steel.

1. Introduction

In quest for eco-friendly corrosion inhibition of metals, the replacement of chromate corrosion inhibitors is of particular interest nowadays [1]. Rare-earth based corrosion inhibitors, vanadium compounds, lithium-based corrosion inhibitors, silica-based corrosion inhibitors and phosphate-based corrosion inhibitors present examples of categories of promising alternatives for a variety of metal substrates [1,2]. In addition, it has been stated that the replacement of chromate corrosion inhibitors will require synergistic combinations of protective chemistries, which, to date, need to be identified and characterized mainly experimentally with, for example, high-throughput methods [3]. Although, recently, efforts are made towards *in silico* studies of corrosion inhibitor synergism [4].

Silicates are known to form complex colloidal structures in aqueous solutions with characteristic physicochemical properties such as its equilibrium and reactivity [5]. As such, the protective properties depend highly on the pH and the salt concentration in the solution [5]. Calcium-exchanged silica or calcium ion exchange silica is a basic pigment with a high specific surface area releasing in an efficient and controlled way its inhibitive species that undergo an exchange reaction with aggressive ions (e.g. H^+ and Cl^-), reducing their availability, and leaching calcium ions at the same time. These calcium ions, together with the polysilicate ions, inhibit corrosion by the formation of protective layers on the metallic surface [6,7].

Zinc phosphates are a widely used alternative to chromates but unfortunately have inadequate inhibition performance, related to their low solubility [8–10]. This led to the use of second and third generation, 'modified', phosphate-based inhibitors through the modification of the cationic constituent as well as the anionic part [8,10,11]. These substances exhibit superior anticorrosion behaviour compared to zinc phosphate [8]. Polyphosphates are known to be cathodic corrosion inhibitors which require the presence of oxygen for effective functioning [5]. Modified zinc phosphate pigments, such as zinc aluminium molybdenum orthophosphate hydrate and zinc calcium strontium aluminium orthophosphate silicate hydrate, were found to have superior

* Corresponding author.
E-mail address: m.meeusen@tudelft.nl (M. Meeusen).

https://doi.org/10.1016/j.corsci.2020.108780
Received 13 January 2020; Received in revised form 3 May 2020; Accepted 1 June 2020
Available online 03 June 2020

corrosion protective properties compared to conventional zinc phosphate pigments [2,8]. Furthermore, it has been shown that the combination of silicates and polyphosphates provides a synergistic effect on carbon steel [5].

These systems have been studied extensively with different electrochemical and surface analysis techniques. In our previous paper, we developed a strategy for the study of corrosion inhibitor-containing systems in the time-domain [12]. It was shown that an elaborated approach combining different electrochemical techniques is strictly necessary for a detailed evaluation of the behaviour of corrosion inhibitors in the time-domain. Potentiodynamic polarization (PP) measurements provide mechanistic information on the cathodic and anodic stationary behaviour at discrete moments in time. Open circuit potential (OCP) measurements with superimposed linear polarization resistance (LPR) measurements are a faster and non-invasive alternative providing time-resolved information in terms of the polarization resistance (R_p) over immersion time in an inhibitor-containing aqueous solution. However, any mechanistic information is lost and frequency-resolved information cannot be obtained. Electrochemical impedance spectroscopy (EIS) measurements can, on top of providing overall performance information of an inhibitor-containing electrochemical system over time, also provide information about the corrosion inhibitive mechanism in the frequency domain. Nevertheless, only stationary information is obtained since time-invariance is assumed de facto in the technique execution and analysis. Electrochemical noise (EN) measurements, however, can provide non-stationary information in terms of the instantaneous electrochemical current noise (ECN) and electrochemical potential noise (EPN) over time but are insufficient in quantitatively describing the system at specific discrete times of exposure in terms of the noise resistance (R_n). The application of odd random phase electrochemical impedance spectroscopy (ORP-EIS) measurements is strictly necessary to study the time-invariance behaviour of corrosion inhibitor-containing electrochemical systems and evaluate the trustworthiness of the quantitative results obtained from the previously discussed electrochemical techniques. The presence of non-stationarities in the initial stages after immersion is translated in unstable R_p values with significant standard deviation obtained from LPR and EIS. As soon as the corrosion inhibitor-containing system reaches a stationary state, also the R_p values become stable as a function of time. In this paper, this methodology is now applied to study the protection performance of different silica- and phosphate- based corrosion inhibitors and corrosion inhibitor synergy for hot-dip galvanized steel.

2. Experimental details

2.1. Materials and sample preparation

Hot-dip galvanized steel samples were obtained from Tata Steel, IJmuiden The Netherlands, with an average coating mass of 275 g m^{-2} and a nominal composition of the steel substrate and the galvanized coating as presented in Table 1. For all electrochemical techniques the hot-dip galvanized steel samples were then cut to 50 by 30 mm. On these samples, a circular exposed area of 2.01 cm^2 is used for PP, LPR, EIS and ORP-EIS and of 0.28 cm^2 for EN measurements. All results presented are surface area corrected. The hot-dip galvanized steel samples were then alkaline cleaned according to ASTM D 6386-99 [13]. Firstly, the samples are cleaned with acetone in the ultrasonic bath for 5 min. Secondly, the samples are immersed in a 1 M NaOH solution, adjusted to pH 12 with H_3PO_4, for 30 s. Finally, the samples are rinsed with distilled water and dried.

5 Commercially available corrosion inhibitors were selected to perform this study. The first corrosion inhibitor, Novinox®ACE110, is a new generation of modified silica as an alternative to strontium chromate and acquired from SNCZ anticorrosion. The second one, Novinox®XCA02, a calcium exchanged silica, is also acquired from SNCZ anticorrosion. The third corrosion inhibitor, Halox®SW-111, is a strontium phosphosilicate from ICL performance products. The fourth and fifth corrosion inhibitor, Heucophos®CAPP and Zinc Phosphate ZP10, respectively, are a calcium aluminium polyphosphate silicate hydrate and a zinc orthophosphate hydrate provided by Heubach. A 0.05 M NaCl solution was used as a reference for all measurements, relevant for building and construction steel applications. Furthermore, this salt concentration is preferred for future local electrochemical experiments. Based on this reference solution, different corrosion inhibitor-containing solutions were prepared.

X-ray Fluorescence (XRF) analysis was carried out to determine the molar mass of the corrosion inhibitors to make corrosion inhibitor solutions with different molarity and to identify the characteristic elements present in the corrosion inhibitor powders. The measurements on the pressed powders were performed with a Panalytical Axios Max WD-XRF spectrometer and the data evaluation was done with SuperQ5.0i/Omnian software. The main composition of the tested corrosion inhibitors as analysed by XRF is presented in Table 2. XRF analysis on corrosion inhibitor 1 (Novinox®ACE110) revealed mainly silica (88.42 wt%) and phosphorous pentoxide (P_2O_5, 7.12 wt%). Inhibitor 2 (Novinox®XCA02) comprises next to silica (94.06 wt%) also calcium oxide (CaO, 5.40 wt%). Inhibitor 3 (Halox®SW-111) consists primarily of silica (43.74 wt%), calcium oxide (36.08 wt%) and phosphorous pentoxide (12.49 wt%). Inhibitor 4 (Heucophos®CAPP) incorporated silica (34.46 wt%), phosphorous pentoxide (29.40 wt%), calcium oxide (25.89 wt%) and alumina (Al_2O_3, 8.83 wt%) as main components. Inhibitor 5 Zin. (Zinc Phosphate ZP 10) is made up of mainly zinc oxide (ZnO, 60.66 wt%) and phosphorous pentoxide (38.58 wt%) with small traces of silicon (as silica) as characteristic element present.

2.2. Electrochemical techniques

A typical three electrode set-up, consisting of a Ag/AgCl 3 M KCl reference electrode, a stainless steel grid as the counter electrode and the hot-dip galvanized steel sample as the working electrode, was used for the ORP-EIS, PP, OCP with superimposed LPR and EIS experiments. A conventional three electrode set-up with two identical hot-dip galvanized steel working electrodes placed at equal distance at either side of a Ag/AgCl 3 M KCl reference electrode, under open-circuit conditions, was used for the EN experiments. To avoid electromagnetic disturbance form external source, the ORP-EIS, EIS and EN measurement set-up was placed in a Faraday cage.

Table 1
Nominal composition of the hot-dip galvanized steel substrate and the galvanized coating.

steel substrate (ppm)	C	Mn	Si	Al	N	P	S	V	Ti	Cu	Sn	Cr	Ni	Mo	Ca
	440	2120	120	460	27	70	70	10	20	150	20	150	210	20	33
coating (wt%)	Al	Fe	Mg	Zn											
	0.36	0.25	0	rest											

Table 2
Main composition of the 5 commercially available corrosion inhibitors tested as determined by XRF.

Inh #	Tradename	Chemical name	SiO_2 (wt%)	P_2O_5 (wt%)	CaO (wt%)	Al_2O_3 (wt%)	ZnO (wt%)	Other (w%)
1	Novinox®ACE110	Modified silica	88.42	7.12				4.46
2	Novinox®XCA02	Calcium exchanged silica	94.06		5.40			0.54
3	Halox®SW-111	Strontium phosphosilicate	43.74	12.49	36.08			7.69
4	Heucophos®CAPP	Calcium aluminium polyphosphate silicate hydrate	34.46	29.40	25.89	8.83		1.42
5	Zinc Phosphate ZP10	Zinc orthophosphate hydrate		38.58			60.66	0.76

2.2.1. Odd-random phase electrochemical impedance spectroscopy

Measurements were recorded immediately after immersion in solution with and without corrosion inhibitors every 15 min for 24 h. For each system, without or with corrosion inhibitors, the measurement was at least repeated once for reproducibility reasons.

The ORP-EIS experiments were performed with a Matlab controlled set-up consisting of a SP-200 potentiostat from Bio-Logic Science Instruments and a National Instruments PCI-6110 DAQ card. The frequency range was set from 10^{-2} Hz to $2{\cdot}10^{3}$ Hz. The amplitude of the excitation signal was set to 3 mV (2.12 mV root mean square (RMS)) in the case of the hot-dip galvanized steel without corrosion inhibitors and 5 mV (3.54 mV RMS) in the case of hot-dip galvanized steel with corrosion inhibitors, versus the OCP, in order to have a good signal-to-noise ratio and keeping the non-linearities confined meanwhile. The Matlab software to build the odd random phase multisine excitation signal and record the measurements was developed at the Vrije Universiteit Brussel. An in-depth description of this technique can be found elsewhere [14,15].

In order to take the time-effect into account and study the evolution of each respective system towards a 'stable' electrochemical system, i.e. fulfilling the causality, linearity and stationarity condition, hot-dip galvanized steel was intensively monitored with ORP-EIS for 24 h after immersion in each of the corrosion inhibitor-containing solutions. ORP-EIS measurements on hot-dip galvanized steel without corrosion inhibitor were carried out as a reference. Each electrochemical system is discussed separately. In our previous work, we have shown that it is necessary to quantify the ORP-EIS data per frequency decade in order to precisely study the evolution of a corrosion-inhibitor containing system towards stability and correlate this to the (in)stability of different electrochemical processes with different characteristic time-constants [12]. The rigorous approach how the quantitative interpretation per frequency decade was obtained from the qualitative and overall quantitative information can be found in Supplementary Material.

The impedance data, ranging from 10^{-2} Hz to $2{\cdot}10^{3}$ Hz, is first divided into 6 frequency decades. Nevertheless, the highest (10^{3} - $2{\cdot}10^{3}$ Hz) and lowest (10^{-2} – 10^{-1} Hz) frequency decade are not taken into account during interpretation because the former only comprises one tenth of a frequency decade and the latter only contains three data points. The information is then quantified by a numerical integration through interpolation procedure using the trapezoidal rule and subtracting the noise curve form the *noise + nonlinearities* and *noise + non-stationarities* curve, respectively. The resulting individual contributions of the noise, non-linearities and non-stationarities per frequency are then expressed relative to the magnitude of the impedance modulus, which is also quantified through a numerical integration [16].

The multisine impedance measurements and the interpretation of the non-stationarities per frequency decade as a function of time carried out here show how the different systems behave in different frequency regions towards the stabilization of the electrochemical processes and present another time-domain than what is measured with classical EIS. This ORP-EIS time-domain is measured first and is coupled later to how classical electrochemistry is performed later on by clarifying the results from the classical electrochemical methods.

2.2.2. Potentiodynamic polarization

PP curves were acquired after 1.5 h, after stabilization of the OCP, and after 24 h by measuring the cathodic and anodic branch separately on different hot-dip galvanized steel samples and for at least three times per system without or with corrosion inhibitor. The cathodic and anodic branch were measured from +30 mV to −500 mV and −30 mV to +500 mV relative to the OCP, respectively, ensuring a small overlap between both branches around the OCP. A scan rate of 1 mV/s was applied and a measurement point was taken every 0.2 s. The corrosion potential (E_{corr}) and the corrosion current density (i_{corr}) were determined using the Tafel extrapolation procedure. The former was then compared versus the OCP value to evaluate the quality of the extrapolation. The latter was used to calculate the inhibitor efficiency η (%) and the polarization resistance R_p (kΩ cm²) later on. Throughout this work, all results are rounded according to the two-digits rule: the standard deviation is rounded to two significant digits first, and the mean is then rounded to the same number of decimal places as the standard deviation [17,18].

2.2.3. Open circuit potential with superimposed linear polarization resistance

The OCP is monitored continuously for 168 h, while on top performing a superimposed LPR measurements every hour with an amplitude of ± 5 mV versus the OCP with a scan rate of 0.1667 mV/s on at least three samples without or with corrosion inhibitor. The R_p was calculated from the slope from the potential versus current graph at the corrosion potential (E_{corr}) as described in ASTM G3-89 [19]. Based on this, and using the anodic and cathodic Tafel slopes (β_a and β_c) obtained from PP experiments, the corrosion current density (i_{corr}) was calculated [20].

2.2.4. Electrochemical impedance spectroscopy

The EIS measurements were performed with a VMP-300 multichannel potentiostat from Bio-Logic Science Instruments in a frequency range from 10^{5} Hz to 10^{-2} Hz, with 7 points per decade on at least three samples per system without or with corrosion inhibitors. The amplitude of the excitation signal was set to 10 mV versus the OCP. An EIS measurement was carried out every 30 min, for a total duration of 168 h.

2.2.5. Electrochemical noise

EPN and ECN signals were recorded with a Compactstat potentiostat from Ivium Technologies working as potentiometer and zero resistance ammeter (ZRA) on at least three samples per system without or with corrosion inhibitor. The sampling frequency was set to 20 Hz and a low-pass filter of 10 Hz, the Nyquist frequency at this sampling rate, was applied during data recording. The measurement range of the potentiometer was set at 40 mV after removal of the initial DC drift component. The minimum and maximum ranges of the ZRA were automatically selected during the experiments, depending on the dynamic range of the ECN signal locally, with a lower limit of 1 nA and an upper limit of 100 μA. The data were processed using Matlab from Mathworks [21–23].

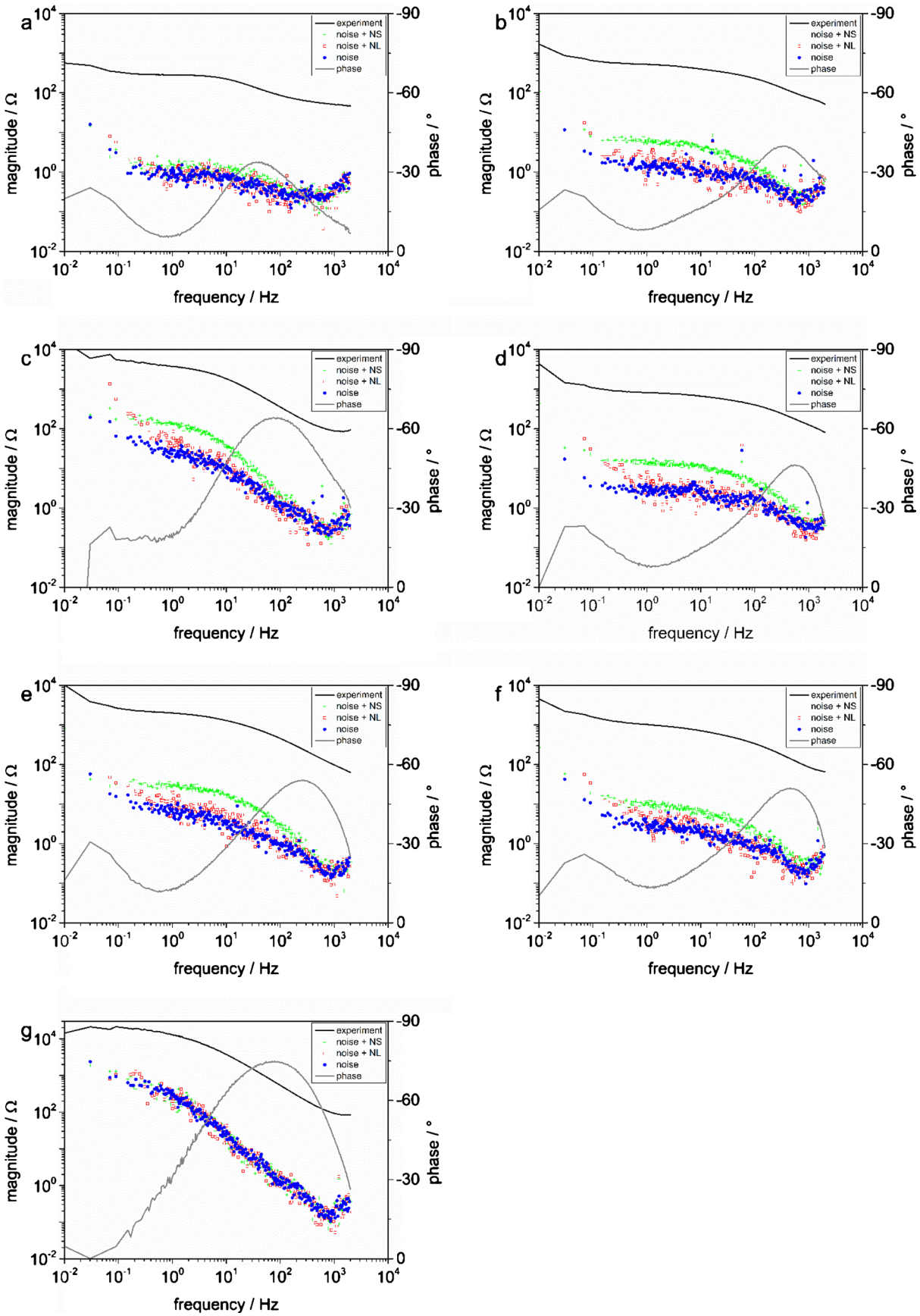

Fig. 1. Bode plots of hot-dip galvanized steel without corrosion inhibitors **(a)**, with Inhibitor 1 (0.5 mM Novinox®ACE110) **(b)**, inhibitor 2 (0.5 mM Novinox®XCA02) **(c)**, inhibitor 3 (0.1 mM Halox®SW-111) **(d)**, inhibitor 4 (0.5 mM Heucophos®CAPP) **(e)**, inhibitor 5 (0.02 mM Zinc Phosphate ZP10) **(f)** and inhibitor 1 + 2 (both 0.5 mM) **(g)** after 1.5 h with the experimental impedance and noise distortion curves.

3. Results and discussion

3.1. Odd-random phase EIS

ORP-EIS is applied as the electrochemical tool to study the time-effect by the evaluation of the non-stationarities per frequency decade over time. Fig. 1 shows the Bode plots, with the magnitude of the impedance modulus (black line), the phase angle (grey line) and the characteristics of the ORP-EIS data, i.e. the curves representing the noise (blue), the noise plus the non-linearities (red) and the noise plus the non-stationarities (green), after 1.5 h of immersion for the system without corrosion inhibitors and the different systems with corrosion inhibitors. The relative contribution of the noise, non-linearities and non-stationarities per frequency decade as a function of immersion time

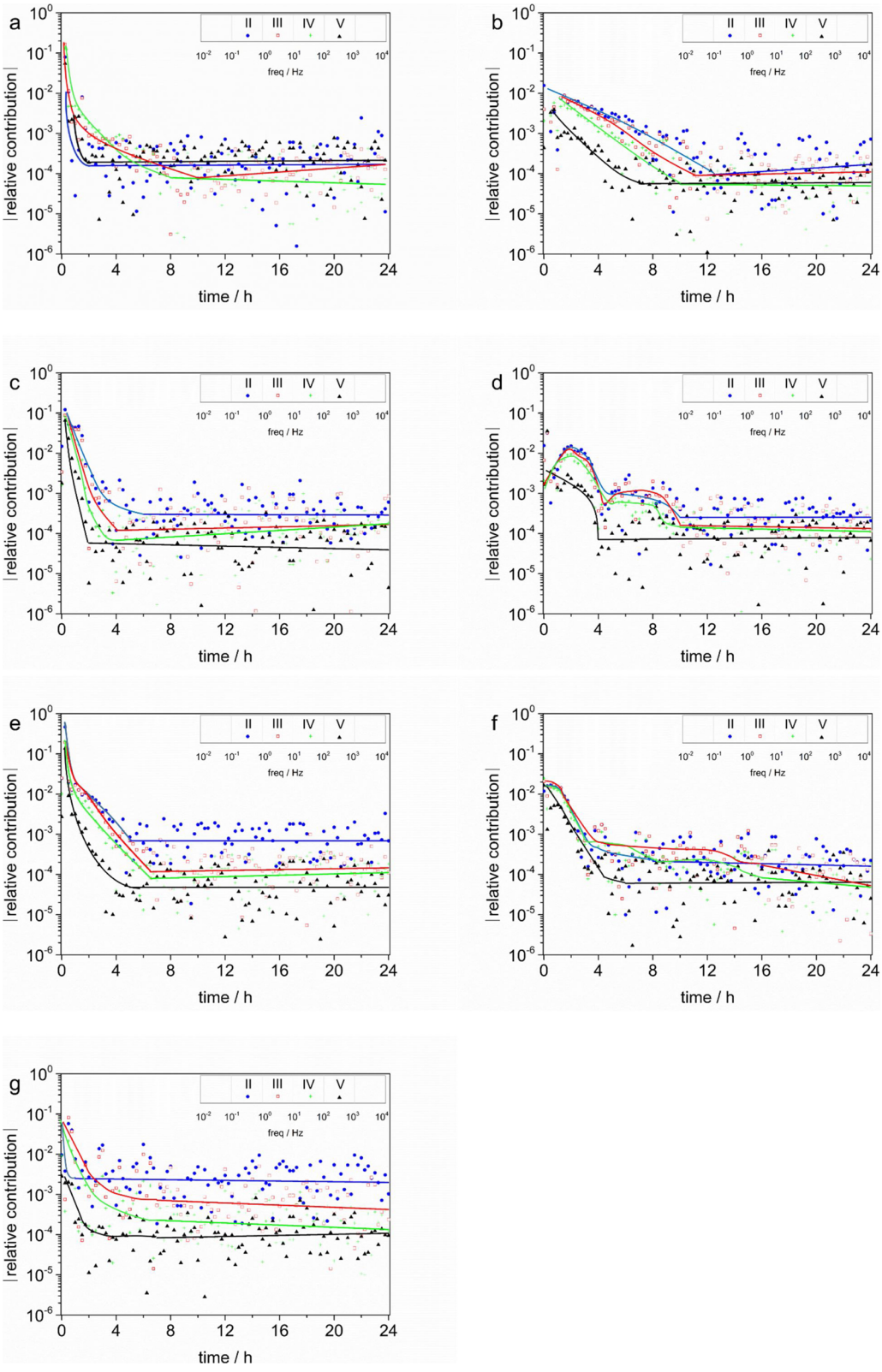

Fig. 2. Evolution of the relative contribution of the non-stationarities for the different frequency decades for hot-dip galvanized steel without corrosion inhibitor (0.05 M NaCl) **(a)**, with Inhibitor 1 (0.5 mM Novinox®ACE110) **(b)**, inhibitor 2 (0.5 mM Novinox®XCA02) **(c)**, inhibitor 3 (0.1 mM Halox®SW-111) **(d)**, inhibitor 4 (0.5 mM Heucophos®CAPP) **(e)**, inhibitor 5 (0.02 mM Zinc Phosphate ZP10) **(f)** and inhibitor 1 + 2 (both 0.5 mM) **(g)** for the first 24 h of immersion, respectively. The blue, red, green and black lines represent the trend line of the non-stationarities in the respective frequency decades (For interpretation of the references to colour in this figure legend, the reader is referred to the web version of this article).

is shown in Fig. 2. As previously remarked, the rigorous approach how the quantitative interpretation per frequency decade was obtained from the qualitative and overall quantitative information can be found in Supplementary Material.

3.1.1. Hot-dip galvanized steel without corrosion inhibitors

From the quantitative interpretation per decade for the system without corrosion inhibitors (Fig. 2a), it can be observed that the contribution of the non-stationarities for all frequency decades decreases with time, although the decrease for the highest and lowest frequency decades (V and II) is more rapidly as compared to the middle frequency decades (IV and III). former stabilize after 2 h while the latter stabilize only after 8 and 10 h. Consequently the system needs to be considered as non-stationary in the first 10 h after immersion. The respective Bode phase angle plot (Fig. 1a) clearly reveals the presence of two time-constants, one in the middle frequency region (10^3-10° Hz, coupled to frequency decades V, IV and III) associated with the corrosion activity related to the effect of the ionic double layer capacitance, and one in the lower frequency region (below 10° Hz, coupled to frequency decade II), associated with the diffusion of the zinc oxidation products to the bulk solution or oxygen reduction [24–28]. This implicates that the electrochemical processes with characteristic time-constants corresponding to the middle frequency region, i.e. the corrosion activity, cause the overall system instability. It needs to be remarked that the distinction between the low-, middle- and high- frequency region is made based on the full frequency spectrum as measured with classical EIS (10^5-10^{-2} Hz), and not on the restricted spectrum measured with ORP-EIS, to avoid misunderstanding later on.

3.1.2. Hot-dip galvanized steel with corrosion inhibitor 1

From the quantitative analysis per frequency decade (Fig. 2b), it can be seen that the contribution of the higher frequency decades decreases more rapidly than the contribution of the middle and lower frequency decades, i.e. frequency decade V reaches a stable value after 7 h, while frequency decades IV and III only reach a stable value after 10 and 11 h and decade II only after 12 h. The accompanying Bode phase plot (Fig. 1b) reveals the presence of two time-constants, one in the middle frequency region (10^3-10^1 Hz, coupled to frequency decades V and IV), related to the corrosion inhibitor protective action and one in the low frequency region (below 10° Hz, coupled to frequency decade II), associated with corrosion activity [29,30]. This implicates that the electrochemical processes with characteristic time-constants corresponding to the middle and lower frequency region cause the overall system instability, meaning that the corrosion inhibitor protective action and the corrosion activity are causing the instability in the case of inhibitor 1.

3.1.3. Hot-dip galvanized steel with corrosion inhibitor 2

From the quantitative interpretation per frequency decade (Fig. 2c) for the system containing corrosion inhibitor 2, it can be seen that all frequency decades decrease rapidly with time, reaching a stable value after 2, 4 and 6 h in the case of the high frequency decade (V), middle frequency decades (IV and III) and low frequency decades (II), respectively. The Bode phase plot (Fig. 1c) again reveals the presence of two time-constants, one in the middle- (10^3-10° Hz, coupled to frequency decades V, IV and III) and one in the low- frequency region (below 10° Hz, coupled to frequency decade II), related to corrosion inhibitor protective action and corrosion activity, respectively [29,30]. This implies that the electrochemical processes related to the corrosion inhibitor protective action stabilize before the corrosion activity, i.e. the charge transfer reaction, stabilizes.

3.1.4. Hot-dip galvanized steel with corrosion inhibitor 3

From this quantitative interpretation per frequency decade (Fig. 2d), it can be observed that the highest frequency decade (V) stabilizes first, after 4 h. The middle frequency decades (IV and III) and the lowest frequency decade (II) all stabilize after 10 h. Yet again, the Bode phase plot (Fig. 1d) reveal the presence of two time-constants with likewise frequency behaviour and physical interpretation as in the case of corrosion inhibitor 1. This indicates that the corrosion inhibitor protective action and the corrosion activity, with characteristic time-constants corresponding to the middle and low frequency region, respectively, prolong the overall system's instability but stabilize after the same time. It can be remarked that the first stabilization plateau, visible in the overall quantitative interpretation, corresponds to the stabilization of the higher frequency decades and the corresponding electrochemical processes.

3.1.5. Hot-dip galvanized steel with corrosion inhibitor 4

From the quantitative interpretation per frequency decade (Fig. 2e), it can be seen that the contribution of the highest (V) and lowest (II) frequency decade decrease more rapidly, reaching a stable value after 5 h, compared to the relative contribution of the middle (IV and III) frequency decades, reaching a stable value after 6.5 h. The Bode phase plots (Fig. 1e) reveal the presence of two time-constants, comparable to corrosion inhibitor 2. This indicates that for the system with corrosion inhibitor 4, the corrosion inhibitor protective action causes the overall system's instability since these frequency decades correspond to the time-constants describing those electrochemical processes. Compared to the system without corrosion inhibitors, it can be concluded that the presence of corrosion inhibitor 4 effectively stabilizes the surface of the hot-dip galvanized steel.

3.1.6. Hot-dip galvanized steel with corrosion inhibitor 5

The quantitative analysis per frequency decade of the system containing corrosion inhibitor 5 shows a remarkable difference in stabilization time of the different frequency decades (Fig. 2f). The highest and lowest frequency decades (V and II) stabilize first, after 6 h and 8 h, respectively. At the same time, the middle frequency decades (IV and III) reach a stabilization plateau more than three orders of magnitude lower compared to the magnitude of the impedance modulus. Nevertheless, after 12 h, the non-stationarities of the middle frequency regions decrease further to eventually more than three orders of magnitude lower than the magnitude of the impedance modulus after 16 h. A similar physical interpretation and frequency behaviour can be made from the Bode phase plot of corrosion inhibitor 5 (Fig. 1f) as for corrosion inhibitor 2. It can be concluded that corrosion inhibitor 5 is ineffective in stabilizing the interface, indicated by the presence of non-stationarities in the middle frequency region accounting for this.

3.1.7. Hot-dip galvanized steel with corrosion inhibitor 1 + 2

Since this research also aimed to study synergistic combinations between corrosion inhibitors, different combinations out of the working corrosion inhibitors were tested for possible corrosion inhibitor synergism. One of the tested corrosion inhibitor combinations, is the system consisting of a combination of inhibitor 1 and 2 (both 0.5 mM). The accompanying Bode phase plot (Fig. 1g) reveals the presence of one broad time-constant ranging from 10^3-10^{-1} Hz, accounting for the corrosion inhibitor protective action and small time-constant below 10^{-1} Hz, accounting for the corrosion activity [29,30]. From the quantitative interpretation per decade (Fig. 2g), it can be seen that the lowest frequency decade (II) stabilizes first after 1 h, while the highest (V) and middle (IV and III) frequency decades stabilize together after 7 h, indicating that the electrochemical processes with characteristic time-constants corresponding to theses frequencies, i.e. the corrosion inhibitor protective action, stabilize after 7 h.

In general, it can be concluded that the system without corrosion inhibitors is behaving non-stationary during the first 10 h after immersion, with the electrochemical processes with characteristic time-constants corresponding to the middle frequency region, i.e. the corrosion activity, prolonging the system's instability. For the system with the silica-based corrosion inhibitors, i.e. corrosion inhibitor 1 and corrosion inhibitor 2, the non-stationarities in the low-frequency region

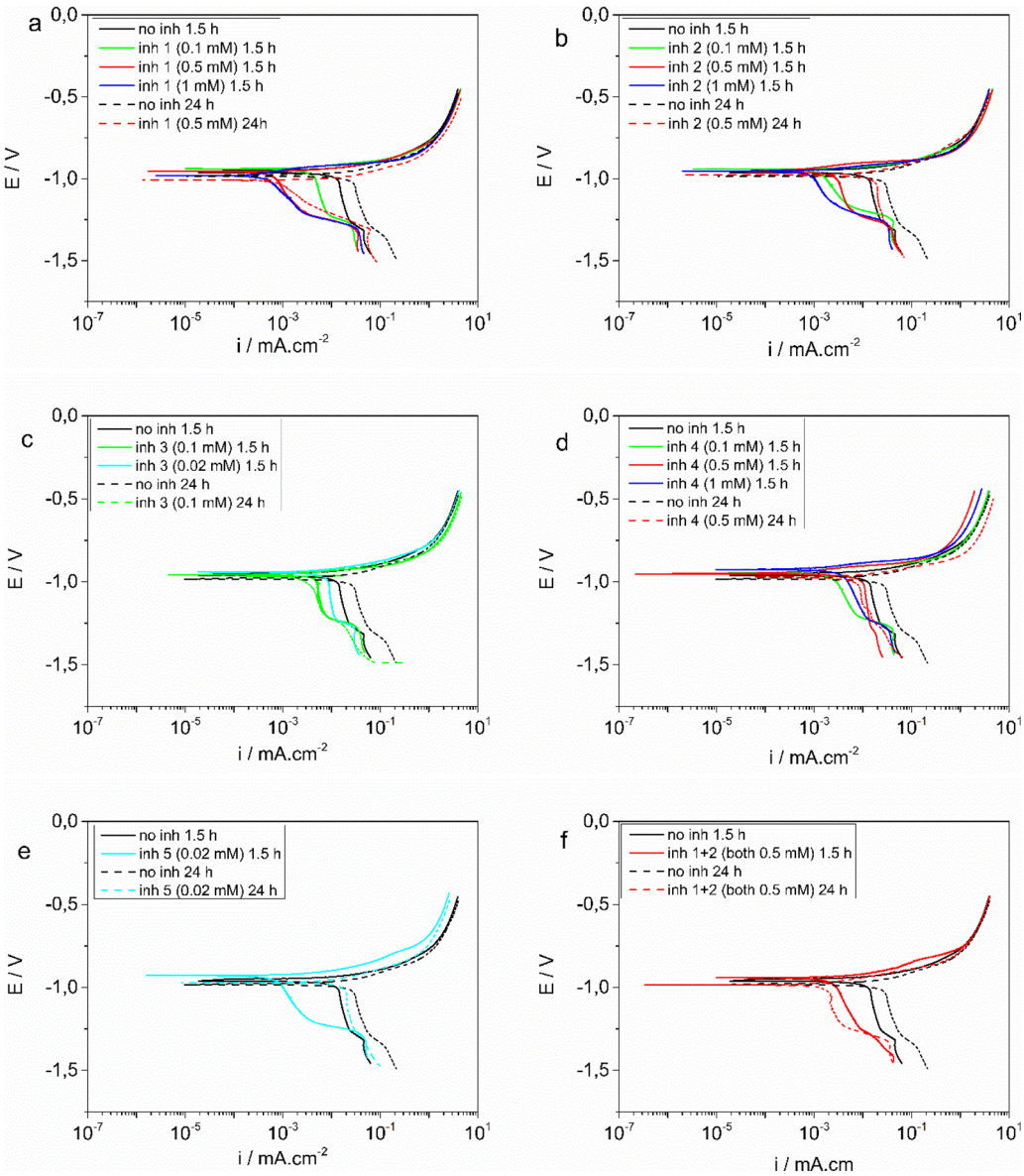

Fig. 3. Potentiodynamic polarization diagram of hot-dip galvanized steel with and without corrosion inhibitors after 1.5 h and 24 h. Inhibitor 1 (Novinox®ACE110) **(a)**; inhibitor 2 (Novinox®XCA02) **(b)**; inhibitor 3 (Halox®SW-111) **(c)**; inhibitor 4 (Heucophos®CAPP) **(d)**; inhibitor 5 (Zinc Phosphate ZP10) **(e)**; inhibitor 1 + 2 **(f)**.

dominate the overall system's instability for 12 h and 6 h, respectively. The combination of corrosion inhibitor 1 and 2 effectively stabilizes the electrochemical interface after 7 h, where the corrosion inhibitor protective action prolongs the system instability, related to the middle frequency region. For the phosphate-based corrosion inhibitors, i.e. corrosion inhibitors 3, 4 and 5, the electrochemical processes with time-constants related to the middle frequency region dominate the system's instability and eventually stabilize after 10 h, 6.5 h and 16 h, respectively. These 'stabilization times' are important to consider when interpreting the electrochemical data obtained from conventional, well-established electrochemical techniques in the subsequent paragraphs.

3.2. Potentiodynamic polarization

Potentiodynamic polarization measurements represent a first well-established conventional electrochemical technique to retrieve information about the working principle and the optimal dosage of corrosion inhibitors. Therefore, the corrosion inhibitor concentration is varied from one measurement to another. The variety of concentrations that is measured depended on the solubility of the respective corrosion inhibitor powders in the 0.05 M NaCl reference solution. Three different concentrations were used for corrosion inhibitors (1, 2 and 4), i.e. 1 mM, 0.5 mM and 0.1 mM, while for inhibitor 3 the concentrations were 0.1 mM and 0.02 mM and for inhibitor 5 only 0.02 mM was used, due to the lower solubility of these corrosion inhibitor compared to the highly soluble corrosion inhibitors 1, 2 and 4.

In Fig. 3, the PP curves for hot-dip galvanized steel with and without corrosion inhibitors after 1.5 h and 24 h are presented. It can be seen that all corrosion inhibitor-containing electrochemical systems after 1.5 h (Fig. 3a-g) show lower cathodic current densities for all tested concentrations as compared to the system without corrosion inhibitors after 1.5 h, but only marginal anodic inhibition. In the case of corrosion inhibitor 1 (Fig. 3a) and corrosion inhibitor 2 (Fig. 3b), the highest concentration tested, i.e. 1 mM, proves to reduce the corrosion current density the most, while in the case of corrosion inhibitor 4 (Fig. 3d), the lowest concentration tested, i.e. 0.1 mM, turns out to reduce the corrosion current density the most. In the case of corrosion inhibitor 3 (Fig. 3c) no difference is observed between the tested concentrations.

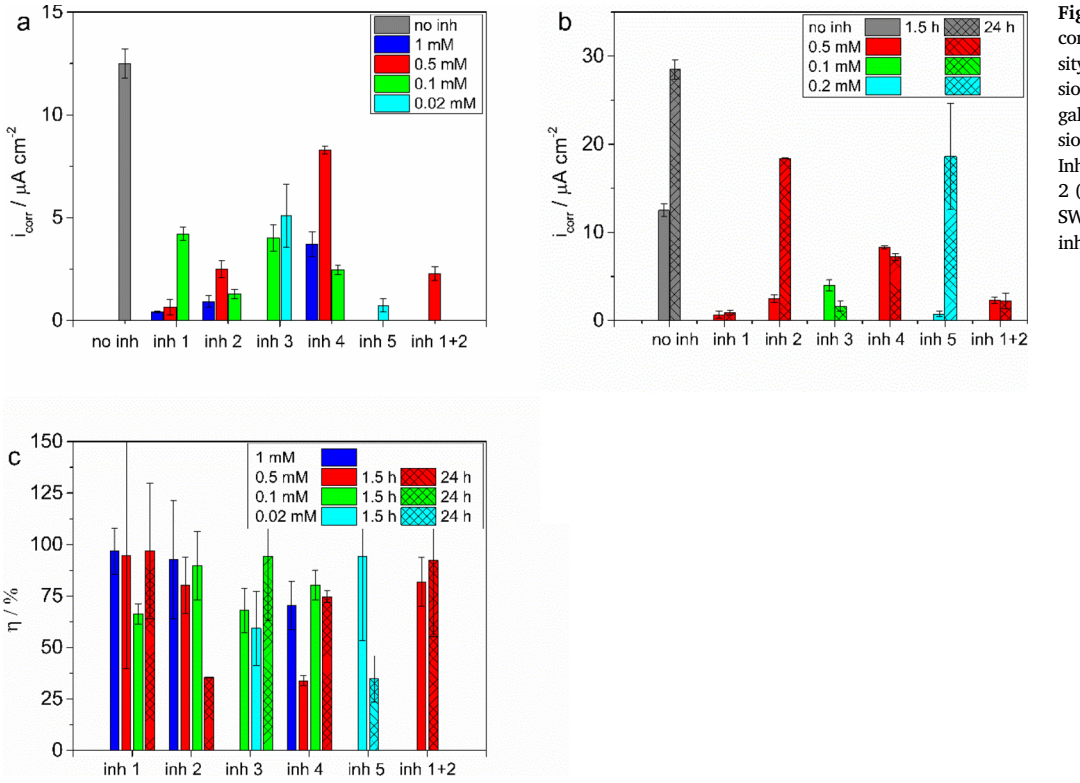

Fig. 4. Corrosion current density a.f.o. concentration **(a)**, corrosion current density a.f.o. immersion time **(b)** and corrosion inhibitor efficiency (η) **(c)** of hot-dip galvanized steel with and without corrosion inhibitors after 1.5 h and 24 h. Inhibitor 1 (Novinox®ACE110); inhibitor 2 (Novinox®XCA02); inhibitor 3 (Halox® SW-111); inhibitor 4 (Heucophos®CAPP); inhibitor 5 (Zinc Phosphate ZP10).

Note that in the case of the system with corrosion inhibitor 5 (Fig. 3e) or corrosion inhibitor 1 and 2 (Fig. 3f) only 1 concentration was tested, so likewise observations cannot be made.

After 24 h, the systems with corrosion inhibitor 1 (Fig. 3a) and inhibitor 4 (Fig. 3d) for a 0.5 mM corrosion inhibitor concentration and the system with corrosion inhibitor 3 (Fig. 3c) for a 0.1 mM concentration show only a slight increase in cathodic current density compared to the situation after 1.5 h for the same concentration, respectively. On the contrary, the system without corrosion inhibitors shows a significant increase in cathodic corrosion current density over the same period of time. For the system with inhibitor 2 (Fig. 3b) and inhibitor 5 (Fig. 3e), for a 0.5 mM and 0.02 mM inhibitor concentration, the cathodic current density shows a remarkable increase over time towards similar values as for the system without corrosion inhibitor. Lastly, the system with corrosion inhibitors 1 and 2 (Fig. 3f) shows a significant decrease in cathodic current density after 24 h, compared to the system without corrosion inhibitors.

In order to make a quantitative comparison between the corrosion inhibitors both over time and as a function of inhibitor concentration, the qualitative observations were translated into corrosion current densities, obtained through Tafel extrapolation [31] and corrosion inhibitor efficiencies (Fig. 4). In Fig. 4a, the corrosion current density (i_{corr}) is shown for the system with and without corrosion inhibitors at different working concentrations after 1.5 h. In the case of the system without corrosion inhibitors, i_{corr} is 12.50 ± 0.71 µA cm^{-2}. The ± values represent the standard deviation on each measurement. For all corrosion inhibitors and all concentrations, i_{corr} is reduced significantly. For the system with corrosion inhibitor 1, inhibitor 2 and inhibitor 5, i_{corr} is reduced the most and decreases to 0.413 ± 0.048 µA cm^{-2}, 0.92 ± 0.28 µA cm^{-2} and 0.74 ± 0.32 µA cm^{-2} in the case of highest corrosion inhibitor concentration measured, respectively. Corrosion inhibitor 3 and inhibitor 4 reduce i_{corr} only by a factor of 2–3. The synergistic combination of corrosion inhibitor 1 and 2 reduces i_{corr} to 2.28 ± 0.33 µA cm^{-2}, almost 6 times lower compared to the system without corrosion inhibitors. The exact corrosion current density values for all systems can be found in Table S1 in Supplementary Material.

However, it needs to be taken into account that all corrosion inhibitor containing systems are still behaving 'unstable', dominated by the presence of non-stationarities, as pointed out by the quantitative analysis per frequency decade of the ORP-EIS data. Consequently, the corrosion current density values presented here should be interpreted as a snapshot in time in the non-stationary regime and should only be compared against each other rather than looking at their exact values.

From the quantitative interpretation per frequency decade of the ORP-EIS data, it has been observed that both the system without and with corrosion inhibitors are behaving 'stable' after 24 h. Fig. 4b shows the evolution of the corrosion current density after 1.5 h and 24 h, respectively. In the case of the reference solution, i_{corr} more than doubles over 24 h. In the case of corrosion inhibitors 1, 2 and 5, a similar observation is made, with an increase in i_{corr} over time. However, the increase in i_{corr} of corrosion inhibitor 1 should be placed in perspective since its increase is small and remains negligible compared to the system without corrosion inhibitors after 24 h. In the case of corrosion inhibitors 3, 4 and the combination of 1 and 2, i_{corr} decreases as a function of time, showing an improved corrosion protection at longer immersion times. It can be concluded that all corrosion inhibitor shown an immediate corrosion protection, but that only corrosion inhibitors 1, 3, 4 and the synergistic combination of corrosion inhibitor 1 and 2 are capable of effectively protecting the hot-dip galvanized steel after 24 h.

To evaluate the effectiveness of the corrosion inhibitors, the corrosion inhibitor efficiency (η) is calculated from the corrosion current density of the inhibited system ($i_{cor(inh)}$) and the reference system (i_{corr}) presented above according to [32]:

$$\eta\,(\%) = \frac{i_{corr} - i_{corr\,(inh)}}{i_{corr}}\, x\, 100 \qquad (1)$$

In Fig. 4c, the corrosion inhibitor efficiency is presented after 1.5 h and 24 h at various concentrations. In the case of corrosion inhibitor 1, inhibitor 2 and inhibitor 5 the highest inhibitor efficiencies are obtained, respectively at their highest concentration measured. Over the course of 24 h, only the efficiency of corrosion inhibitor 1 remains equal, while the corrosion inhibitor efficiencies of inhibitor 2 and

inhibitor 5 drops drastically. The corrosion inhibitor efficiencies of corrosion inhibitor 3 and 4 are relatively low but, however, increase significantly over time. Finally, the system consisting of a 0.5 mM solution of corrosion inhibitor 1 and a 0.5 mM solution of corrosion inhibitor 2 shows an intermediate value after 1.5 h but increases over time. These results reflect of course the observations made earlier regarding the corrosion current density. The exact inhibitor efficiency values for all systems can be found in Table 2 in Supplementary Material.

In the case of inhibitor 1, it needs to be noted that although the corrosion current density increased over time, the inhibitor efficiency increased. This is due to the difference in corrosion current density of the system without corrosion inhibitors after 1.5 h and 24 h, which increased by 128 %. Therefore, only a small decrease or even increase in corrosion current density of the corrosion inhibitor containing system could lead to an efficiency increase and an associated misinterpretation. This indicates that all results have to be placed in the right perspective.

It can be concluded that that all corrosion inhibitor-containing systems, as well as the combination of corrosion inhibitor 1 and 2 showed lower cathodic current densities compared to the system without corrosion inhibitors and only marginal anodic inhibition, indicating cathodic type corrosion inhibitors. Corrosion inhibitor 1 and corrosion inhibitor 3 experience a positive effect of concentration, i.e. an increased inhibitor concentration reduces i_{corr}. For corrosion inhibitor 2 and 4, the highest (1 mM) and lowest (0.1 mM) concentrations tested reduce i_{corr} the most. For the systems containing corrosion inhibitors 5 and the combination of corrosion inhibitor 1 and 2, only one concentration was tested, which effectively reduced i_{corr}. Over time, when comparing the results after 24 h and 1.5 h, only in the case of corrosion inhibitors 3 and 4 i_{corr} is reduced while for corrosion inhibitors 2 and 5, i_{corr} has increased significantly, similarly to the situation without corrosion inhibitors. For corrosion inhibitors 1 and the combination of corrosion inhibitors 1 and 2, comparable i_{corr} are observed. This is all reflected in the corrosion inhibitor efficiencies. These differences in i_{corr} at discrete times in the corrosion inhibitive solutions stress again the importance of studying the electrochemical behaviour of each system as a function of immersion time.

At this point, it has been decided to continue with the 0.5 mM concentrations for corrosion inhibitors 1, 2, 4 and the combination of 1 and 2 and a 0.1 mM and 0.02 mM concentration for corrosion inhibitor 3 and 5, respectively. The former has been chosen to allow a comparison between corrosion inhibitors 1 and 2 on one hand and the combination of corrosion inhibitors 1 and 2 on the other hand. The latter is selected because of efficiency and solubility reasons.

3.3. Open circuit potential with superimposed linear polarization resistance

In the previous section, discrete electrochemical information about the corrosion inhibitor- containing system was gathered by means of potentiodynamic polarization experiments. In order to assess continuous, time-resolved information about the performance of the system over longer times after immersion with and without the presence of corrosion inhibitors, continuous OCP measurements with superimposed LPR measurements every hour were carried out for 168 h. From the slope of the potential versus current plot for every hour, the R_p can be calculated and as such monitored every hour.

Fig. 5 shows the R_p values and their standard deviation of the hot-dip galvanized steel with and without corrosion inhibitors over time, presented separately for the phosphate- (Fig. 5a-b) and silica- based (Fig. 5c-d) corrosion inhibitors. It can be seen that for the hot-dip galvanized steel without corrosion inhibitors (Fig. 4a), the R_p decreases rapidly in the first 10 h. Note also the relatively high absolute error on the R_p values in the first 10 h. This, together with the unstable R_p values during the initial 10 h after immersion can be explained by the presence of the non-stationarities for the same duration and a consequently 'unstable' system which is directly reflected here. Eventually the R_p values continue to decrease over the course of the measurement.

In the case of hot-dip galvanized steel with corrosion inhibitor 3 (Fig. 5a-b), the R_p decreases strongly in the first 10 h followed by a more gradual decrease. The transition from the strong to the more gradual decrease corresponds to the stabilization time of the system as previously observed by the quantitative interpretation per frequency decade of the OPR-EIS data. Following this gradual decrease, a gradual increase is visible to values almost three times higher as compared to the hot-dip galvanized steel without corrosion inhibitor. For corrosion inhibitor 4 (Fig. 5a-b), the R_p decreases slightly in the first 7 h after immersion. At the same time the contribution of the non-linearities stabilizes and the system can be considered fully stable. Similar to corrosion inhibitor 3, a gradual increase is apparent afterwards to values also almost three times higher as compared to the system without corrosion inhibitor. The R_p of hot-dip galvanized steel with corrosion inhibitor 5 (Fig. 5a-b) is more than 10 times higher as compared to the system without corrosion inhibitors at the start, indicating imminent protective action. However, the R_p decreases initially strongly and afterwards more gradually over the course of the measurement, to comparable values for what was observed for corrosion inhibitors 3 and 4. Yet again, the initial strong decrease in the first 16 h with corresponding unstable R_p values with high absolute error could be related to the 'unstable' behaviour of the electrochemical system at these times as shown by the ORP-EIS interpretation per frequency decade.

For the system with corrosion inhibitors 1, 2 and the combination of corrosion inhibitors 1 and 2 a similar observation can be made. For corrosion inhibitors 1 and 2 (Fig. 5c-d), the R_ps decrease initially strongly in the first 12 and 6 h after immersion, respectively, and more gradually in the following hours. Afterwards a gradual increase is noticeable for both corrosion inhibitor 1 and 2. The behaviour of the hot-dip galvanized steel with equal combination of corrosion inhibitor 1 and 2 (Fig. 5c-d) is furthermore remarkable. The R_p right at the start is more than 15 times higher than the system without corrosion inhibitors. Afterwards the R_p decreases initially strongly in the first 7 h, eventually more gradually towards 68 h and remains approximately constant for the rest of the measurement. Here again, the quantitative interpretation of the ORP-EIS data per frequency decade indicated that the systems with corrosion inhibitor 1, 2 and the combination of 1 and 2 behave non-stationary during the initial 12, 6 and 7 h, respectively, which is reflected in the unstable values with relatively high absolute error in these timeframes and depicts the uncertainty on the results acquainted there. The exact polarization resistance values at these characteristic times obtained through LPR for all systems can be found in Table S3 in Supplementary Material.

Similarly to our previous paper, a comparison can be made between the results obtained from LPR and the results obtained from PP previously in terms of the i_{corr} [12]. Starting from the R_p from LPR after 1.5 h, calculated as the average from the respective values after 1 and 2 h, and 24 h, and the anodic and cathodic slopes of the Tafel plot (β_a and β_c, respectively), i_{corr} can be calculated according to the Stern-Geary equation [33]:

$$i_{corr} = \frac{\beta_a \cdot \beta_c}{2.3\,(\beta_a + \beta_c)\,R_p} \quad (2)$$

These parameters and the resulting i_{corr} values are summarized in Table 3. Comparison of these values with the previously obtained values from PP show that there is in general no agreement between the values obtained through both techniques, not only for results after 1.5 h, when all systems are still behaving 'unstable', but also after 24 h when all systems are behaving fully 'stable'. Only for the system without corrosion inhibitor and the system with corrosion inhibitor 5 an agreement is found in both the trend and the i_{corr} values over time.

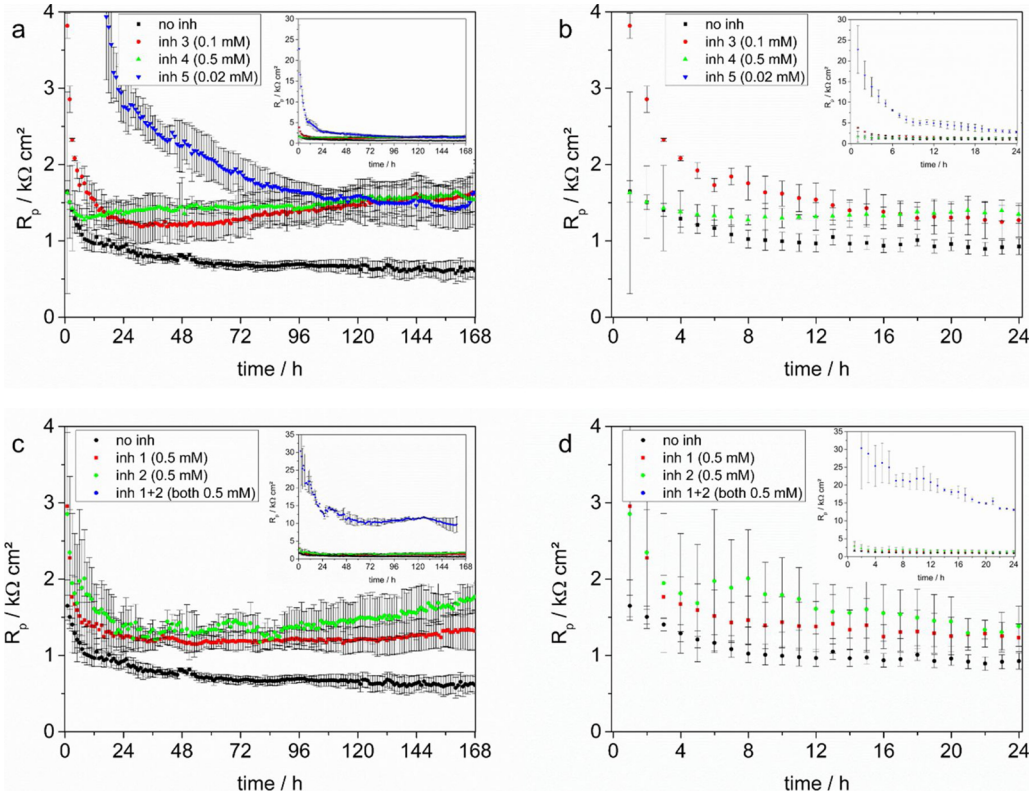

Fig. 5. Polarization resistance (R_p) results and their standard deviation obtained from linear polarization resistance measurements of hot-dip galvanized steel without corrosion inhibitor (0.05 M NaCl), with inhibitor 3 (0.1 mM Halox SW111), inhibitor 4 (0.5 mM Heucophos Capp) and inhibitor 5 (0.02 mM Zinc Phosphate ZP10) **(a)** and **(b)** and with inhibitor 1 (0.5 mM Novinox ACE110), inhibitor 2 (0.5 mM Novinox XCA02) and inhibitor 1 + 2 (both 0.5 mM) **(c)** and **(d)** for 168 h.

Table 3
Tafel Parameters from PP and R_p from LPR for the determination of i_{corr} using Stern-Geary.

	time	R_p (kΩ cm²)	std. dev. (kΩ cm²)	β_a (V/dec)	β_c (V/dec)	i_{corr} (μA cm^{-2})	std. dev. (μA cm^{-2})
no inh	1.5 h	1.58	0.12	0.059	0.084	15.1	1.1
	24 h	0.93	0.11	0.109	1.208	46.8	5.5
Inh 1	1.5 h	2.62	0.80	0.038	0.410	5.8	1.8
	24 h	1.23	0.18	0.036	0.211	10.8	1.6
Inh 2	1.5 h	2.6	1.2	0.054	0.893	8.5	3.9
	24 h	1.39	0.26	0.098	3.192	29.7	5.5
Inh 3	1.5 h	3.34	0.17	0.026	0.949	3.32	0.17
	24 h	1.27	0.22	0.042	0.158	11.3	1.9
Inh 4	1.5 h	1.57	0.90	0.045	0.206	10.2	5.8
	24 h	1.35	0.12	0.079	0.158	16.9	1.5
Inh 5	1.5 h	19.7	4.6	0.035	0.453	0.72	0.17
	24 h	2.76	0.21	0.099	2.574	15.0	1.1
Inh 1 + 2	1.5 h	38	17	0.040	0.545	0.42	0.19
	24 h	13.10	0.23	0.055	15.419	1.802	0.031

Nevertheless, a complete independent comparison is impossible, since kinetic parameters from the Tafel extrapolation need to be used to calculate i_{corr} from R_p obtaind through LPR measurements.

It can be concluded that corrosion inhibitor 5 provides immediate corrosion protection significantly higher than corrosion inhibitor 3 and corrosion inhibitor 4. Over the course of the measurement, the R_p of corrosion inhibitor 5 decreases gradually while for corrosion inhibitors 3 and 4, the R_p increases gradually. Eventually, after 168 h, an R_p almost three times higher than what is observed for the system without corrosion inhibitor is observed for all three corrosion inhibitor-containing electrochemical systems. In the case of corrosion inhibitor 1 and 2, a similar trend is observed with an initial decrease in R_p during the first 2 days and eventually a gradual increase to values two to three times higher as compared to the system without corrosion inhibitor. The LPR results for the system with both corrosion inhibitor 1 and corrosion inhibitor 2 indicate that a synergistic effect is observed. After 168 h, an R_p more than three times higher than the sum of the R_ps of corrosion inhibitor 1 and corrosion inhibitor 2, is observed. Moreover, it needs to be remarked that in the beginning, for both the system without corrosion inhibitors and the systems with corrosion inhibitors, an evolution in terms of an increase or decrease in R_p is observed, while at a certain moment, all systems show stable R_p values. However, the point in time where this transition occurs is different from system to system and is related to the 'stability' of the electrochemical system as studied by the quantitative interpretation per frequency decade of the ORP-EIS data.

3.4. Electrochemical impedance spectroscopy (EIS)

EIS was used to provide not only time-resolved information but also frequency-resolved information on the electrochemical characteristics of hot-dip galvanized steel with and without corrosion inhibitors over time. Since a correct and trustworthy EIS measurement requires the fulfilment of the causality, linearity and stationarity condition, the

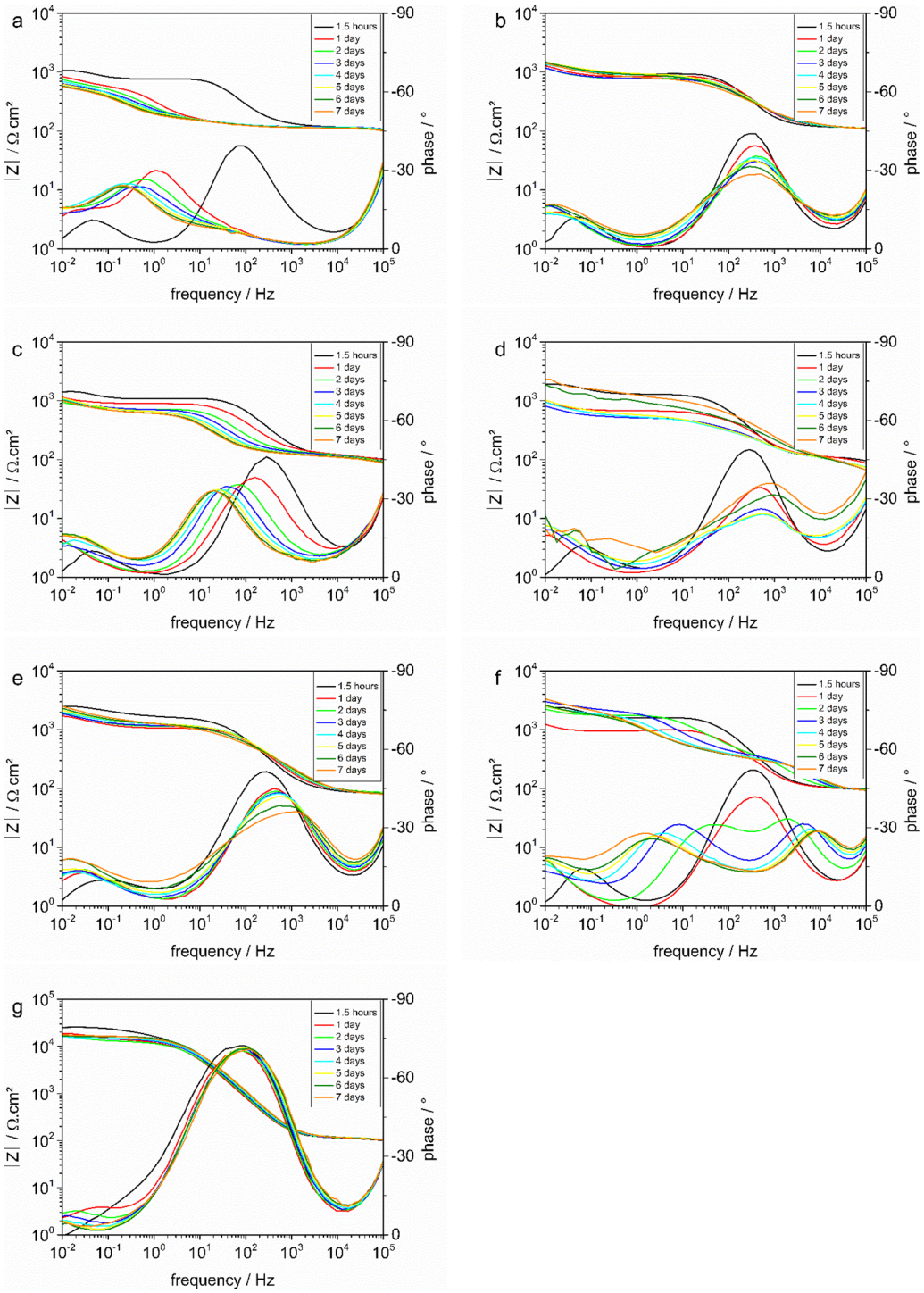

Fig. 6. EIS bode plots for hot-dip galvanized steel with and without corrosion inhibitors every 24 h for 168 h. Without corrosion inhibitor (0.05 M NaCl) **(a)** Inhibitor 1 (0.5 mM Novinox ACE110) **(b)**; inhibitor 2 (0.5 mM Novinox XCA02) **(c)**; inhibitor 3 (0.1 mM Halox SW111) **(d)**; inhibitor 4 (0.5 mM Heucophos Capp) **(e)**; inhibitor 5 (0.02 mM Zinc Phosphate ZP10) **(f)**; inhibitor 1 + 2 (both 0.5 mM) **(g)**.

quantitative interpretation of the ORP-EIS data serves as the basis for the EIS data interpretation providing an electrochemical 'stability' criterion [14].

Fig. 6 shows the Bode plots of the different systems every day up to 1 week after immersion. In the case of the hot-dip galvanized steel without corrosion inhibitors (Fig. 6a), the Bode plots show a remarkable decrease in the impedance modulus of the middle frequency region (10^3–10° Hz) and a gradual decrease in the low frequency region (10°-10^{-1}) with time. In the associated phase plots, two time-constants can be distinguished, one in the middle frequency region and one in the lower frequency region. As previously stated, these can be associated with the corrosion activity, related to the effect of the ionic double layer capacitance and the diffusion of the zinc oxidation products to the bulk solution or oxygen reduction [24–28]. Connected to the decrease in impedance modulus in the middle and low frequency regions is a decline and shift of the phase angle of the first time-constant towards lower frequencies and a decline of the phase angle of the second time-constant. This can be associated to a decreased corrosion resistance of the system without corrosion inhibitors.

The Bode phase plots of all corrosion inhibitor-containing

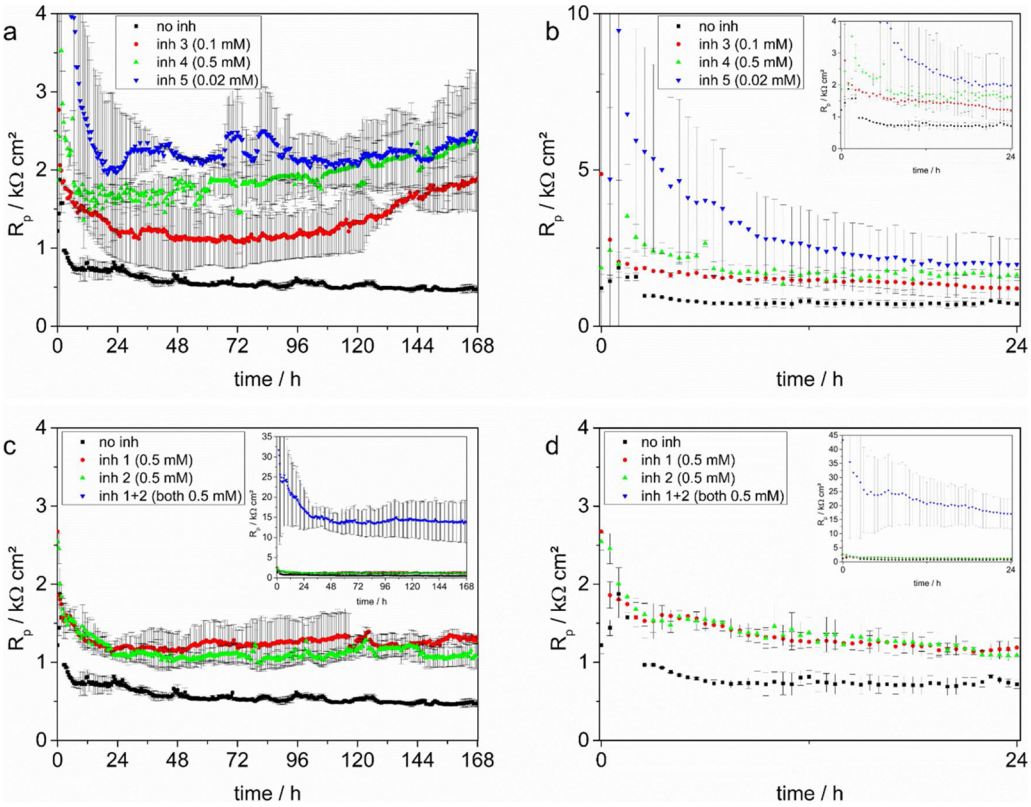

Fig. 7. Polarization resistance (R_p) results and their standard deviation obtained from electrochemical impedance spectroscopy measurements of hot-dip galvanized steel without corrosion inhibitor (0.05 M NaCl), with inhibitor 3 (0.1 mM Halox SW111), inhibitor 4 (0.5 mM Heucophos Capp) and inhibitor 5 (0.02 mM Zinc Phosphate ZP10) **(a)** and with inhibitor 1 (0.5 mM Novinox ACE110), inhibitor 2 (0.5 mM Novinox XCA02) and inhibitor 1 + 2 (both 0.5 mM) **(b)** for 168 h.

electrochemical systems obtained with EIS clearly reveal the presence of two time-constants, likewise the Bode plots obtained with ORP-EIS discussed earlier (Fig. 1 and Supplementary Material): one in the middle frequency region and on in the low frequency region, associated with corrosion inhibitor protective action and corrosion activity, respectively [29,30]. In the case of inhibitor 1 and inhibitor 4 (Fig. 6b,e), the middle frequency time-constant decreases over time and shifts slightly to higher frequencies. In the case of corrosion inhibitor 2 (Fig. 6c), a similar decrease is noticeable, but now coupled to a shift to lower frequencies, associated with reducing inhibitor protective action on the surface. In the case of corrosion inhibitor 3 (Fig. 6d) the middle frequency time-constant decreasing initially but eventually increases and shifts towards higher frequency, indicating the occurrence of corrosion protective action on the surface. In the case of corrosion inhibitor 5 (Fig. 6f) the mid-frequency time-constant broadens over time and eventually, after 2 days, two time-constants can be differentiated here. Additionally to the time-constant in the low-frequency region (10°–10^{-1}) and mid-frequency region (10^{3}–10° Hz), a third time-constant appears in the higher frequency region (10^{4}-10^{3} Hz). The low-frequency time-constant increases over time, while the mid-frequency time-constant decreases and shifts to lower frequencies. The high frequency time-constant shifts to higher frequencies however over the course of 168 h, indicating increased corrosion protection over time. In the case of corrosion inhibitor 1 and inhibitor 2 (Fig. 6g) both time-constants undergo only little change over the course of the measurement indicating immediate- and long-term corrosion protective properties compared to the system without corrosion inhibitor.

The Bode magnitude plots of all single corrosion inhibitor systems (Fig. 6b-f) show a similar trend over the course of 168 h with an initial gradual decrease in the impedance modulus of the middle frequency region, followed by a stabilization period. Eventually, the impedance modulus in the middle frequency region decreases further (inhibitor 1 and 2) or increases slightly (inhibitor 3, 4 and 5). The Bode magnitude plot of the system containing both corrosion inhibitor 1 and 2 (Fig. 6g) shows no relevant changes in the middle frequency region over time. The impedance modulus in the low frequency region decreases initially for all corrosion inhibitor systems (Fig. 6b-g) and stabilizes afterwards. In the case of corrosion inhibitor 1, 3, 4 and 5 an increase is noticeable towards the end of the measurement.

In order to evaluate the consistency between the results obtained from the different macroscopic electrochemical techniques, the R_p values of the EIS measurements are calculated from the real component of the impedance at maximum and minimum frequency, i.e. 100 kHz and 10 mHz, according to [34–36]:

$$R_p = Z'(0) - Z'(\infty) \tag{3}$$

Fig. 7 displays the evolution of the R_p with their standard deviation obtained from EIS measurements for the system with and without corrosion inhibitors over time, shown separately for the phosphate- (Fig. 7a-b) and silica- based (Fig. 7c-d) corrosion inhibitors.

For the system without corrosion inhibitors (Fig. 7a-b), the R_p decreases strongly in the first 10 h after immersion. This time corresponds to the 'stabilization' time of the electrochemical system, i.e. the time to reach a linear and stationary system. In the following hours, the R_p decreases more slowly.

In the case of corrosion inhibitor 3 (Fig. 7a-b), the R_p after 1 h is comparable to the R_p of the system without corrosion inhibitor after the same time. Nevertheless, the R_p decreases strongly initially and eventually more slowly, in the first 10 and 24 h after immersion, respectively. The transition from the strong decrease with unstable values to a more gradual decrease corresponds yet again to the moment in time the system reaches a 'stable' state. The R_p of the system with corrosion inhibitor 4 (Fig. 7a-b) decreases rapidly in the first 6.5 h after immersion, corresponding to the point in time where the system behaves 'stable'. Next, its value starts to increase gradually again over the rest of the measurement. For the system with corrosion inhibitor 5 (Fig. 7a-b), the R_p value at the start is substantially higher as compared to the system without corrosion inhibitors, but in addition the decrease in the initial stages after immersion is more rapid.

It can be seen that the system with corrosion inhibitor 1 behaves

similarly to the system with corrosion inhibitor 2 (Fig. 7c-d). Their R_p values decrease strongly in the first 12 and 6 h after immersion, respectively. Afterwards the R_p remains approximately equal with time for the rest of the measurement. At all times, the R_ps are well above the R_p of the hot-dip galvanized steel without corrosion inhibitor. The R_p of the system with equal combination of corrosion inhibitor 1 and corrosion inhibitor 2 (Fig. 7c-d) decreases strongly in the first 7 h after immersion. From this point on, the R_p values become more stable with lower absolute error, corresponding to the stabilization of the electrochemical system after 7 h. Afterwards, the R_p values decrease gradually over the course of the measurement. Nevertheless, the system consisting of equal amounts of corrosion inhibitor 1 and corrosion inhibitor 2 shows superior behaviour compared to both the system with corrosion inhibitor 1, corrosion inhibitor 2 and the system without corrosion inhibitors. Afterwards the R_p decreases strongly, reaching an approximately stable value after 48 h. The exact polarization resistance values at these characteristic times obtained through EIS for all systems can be found in Table S3 in Supplementary Material.

It can be concluded for corrosion inhibitors 3, 4 and 5 that immediate corrosion protection is observed, indicated by the increase in R_p right at the start after immersion as compared to the system without corrosion inhibitors. During the first 24 h the R_p decreases strongly. Afterwards, the R_p gradually increases again towards 2 kΩ cm^2, approximately 4 times higher compared to the 0.50 kΩ cm^2 observed for the system without corrosion inhibitors. Corrosion inhibitors 1 and 2 show a similar trend with an initial decrease and eventually a gradual increase towards 168 h. At that stage, the polarization resistance is more than two times higher as compared to the system without corrosion inhibitors. The system with both corrosion inhibitor 1 and corrosion inhibitor 2 behaves superior to its individual constituents and reaches an R_p of 14.0 ± 5.0 kΩ cm^2 after 168 h, more than 5 times higher than the sum of its constituents, 1.278 ± 0.049 kΩ cm^2 and 1.08 ± 0.16 kΩ cm^2, respectively. Based on these observations it may be concluded that there definitely exists a synergistic combination of corrosion inhibitor 1 and corrosion inhibitor 2.

Yet again, a similar observation can be made regarding the evolution of the R_p values over time, similar to the R_p values obtained from LPR measurements. In the beginning, a decrease and/or increase is noticeable but after a certain time, a stable R_p value is obtained for the remaining of the measurement, related to the stabilization times observed from the ORP-EIS quantitative interpretation per frequency decade.

3.5. Electrochemical noise

EN measurements were applied as an analysis technique able to process non-stationary data, compared to the previously applied stationary electrochemical techniques and were performed continuously for 24 h after immersion of the hot-dip galvanized steel in the solution with or without corrosion inhibitor. To make a comparison with the other electrochemical techniques in this work, the EPN and ECN data are divided into windows of 1 h. Through a discrete wavelet transform (DWT) procedure, the DC drift component for each of the time windows is removed [22]. The noise resistance (R_n) can then be calculated by dividing the standard deviation of the EPN by the standard deviation of the ECN according to [37]:

$$R_n = \frac{std\ (EPN)}{std\ (ECN)} \quad (4)$$

This R_n is then normalized by the area of the working electrode, which is 0.28 cm^2 for EN measurements. It has been chosen to use this electrochemical parameter because of its correspondence with the polarization resistance R_p [38]. Fig. 8 shows the R_n values and their standard deviation of the hot-dip galvanized steel with and without corrosion inhibitors in the first 24 h after immersion, shown separately for the phosphate- (Fig. 8a) and silica- based (Fig. 8b) corrosion

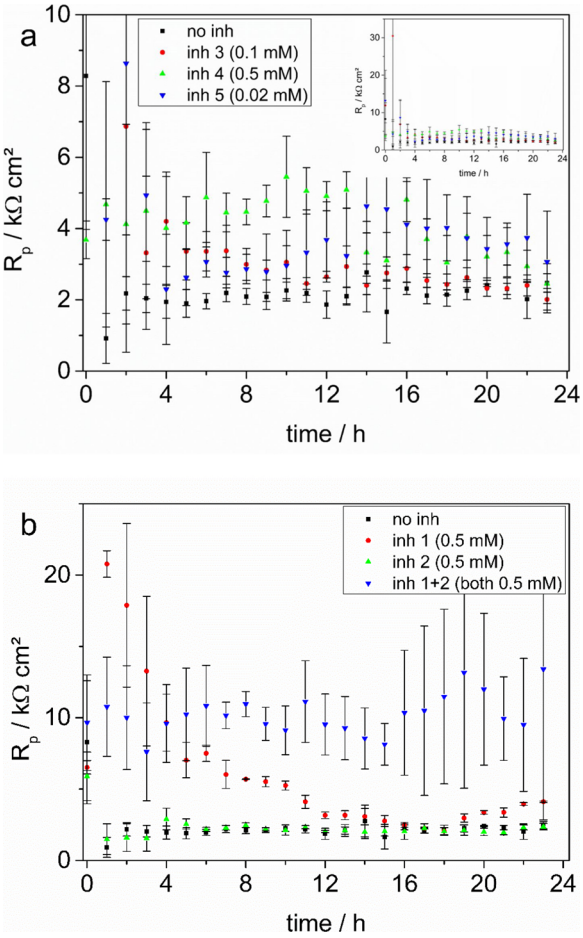

Fig. 8. Noise resistance (R_n) results and their standard deviation obtained from electrochemical noise measurements of hot-dip galvanized steel without corrosion inhibitor (0.05 mM NaCl), with inhibitor 3 (0.1 mM Halox SW111), inhibitor 4 (0.5 mM Heucophos Capp) and inhibitor 5 (0.02 mM Zinc Phosphate ZP10) **(a)** and with inhibitor 1 (0.5 mM Novinox ACE110), inhibitor 2 (0.5 mM Novinox XCA02) and inhibitor 1 + 2 (both 0.5 mM) **(b)** in the first 24 h after immersion.

inhibitors. It should be noted that the indicated times correspond to the starting times of the respective windows. For the system without corrosion inhibitors (Fig. 8a), it can be seen that the R_n decreases in the first 2 h and remains stable afterwards. In the case of hot-dip galvanized steel with corrosion inhibitor 3, the R_n decreases gradually in the first 11 h of immersion. Afterwards, the R_n remains at a constant level, slightly higher compared to what was observed for the hot-dip galvanized steel without corrosion inhibitor. For the system with corrosion inhibitor 4, the R_n increases gradually in the first 10 h after immersion. Afterwards, the R_n decreases again to a value, comparable to what was observed for the hot-dip galvanized steel without corrosion inhibitors after the same time. In the case of the hot-dip galvanized steel exposed to the solution containing corrosion inhibitor 5, the R_n decreases rapidly in the first 4 h after immersion, comparable to the system without corrosion inhibitors. Afterwards, R_n increases again over time to a maximum after 14 h of immersion before decreasing again towards the end of the measurement. Although a higher value is always obtained compared to the situation without corrosion inhibitor present, no stable R_n value is obtained.

A similar observation can be made for the systems containing corrosion inhibitor 1, corrosion inhibitor 2 and the synergistic combination of corrosion inhibitor 1 and 2. It can be seen that (Fig. 8b) there is no effect of corrosion inhibitor 2 on R_n, with similar values as for the hot-dip galvanized steel without corrosion inhibitors. For the system with

corrosion inhibitor 1 however, a noticeable increase in R_n is visible after 1 h of immersion. In the following stages, R_n decreases, before gradually increasing again. In the case of the hot-dip galvanized steel with both corrosion inhibitor 1 and corrosion inhibitor 2, it can be seen that the R_n is stable throughout the measurement with an average value well above the sum of its constituents, which clearly states the synergistic effect of the two corrosion inhibitors after 5 h up to 24 h after immersion. In the first 4 h after immersion, however, the R_n of the hot-dip galvanized steel with corrosion inhibitor 1 exceeds the R_n of the combination of inhibitor 1 and 2. The exact noise resistance values at these characteristic times obtained through EN for all systems can be found in Table S3 in Supplementary Material.

It has to be remarked that the local amplitude in the DC drift of an EN signal provides information about (non)-stationarity of the electrochemical system. Therefore, the EN analysis technique is not expected to be directly affected by the 'stabilization' time and non-stationary behaviour, as determined from the quantitative interpretation per frequency decade from the ORP-EIS data. Nevertheless, the relatively high absolute errors on the first R_n values are due to the non-stationary behaviour which affects the DWT procedure used for DC drift removal [12].

It can be concluded that in the case of the phosphate-based corrosion inhibitors (inhibitors 3, 4 and 5), fluctuations in noise resistance are observed over the course of the measurement. After 24 h, the noise resistance reaches a value only slightly higher compared to the hot-dip galvanized steel without corrosion inhibitors. In the case of the silica-based corrosion inhibitors (inhibitors 1 and 2), corrosion inhibitor 1 only increases the noise resistance in the initial stages after immersion and corrosion inhibitor 2 has a comparable noise resistance to the system without corrosion inhibitors. In the case of both corrosion inhibitor 1 and 2, a remarkable increase in the noise resistance is observed for the entire measurement, approximately 5 times higher than for the case without corrosion inhibitors.

3.6. Comparison of different corrosion inhibitors with different electrochemical techniques in the time-domain

In the previous paragraphs, different macroscopic electrochemical techniques were applied to study the protective action of different corrosion inhibitors for hot-dip galvanized steel and their results were interpreted according to the stability of the respective electrochemical systems as determined from the quantitative interpretation per frequency decade from ORP-EIS data. In this paragraph, all results obtained from the different macroscopic electrochemical techniques are presented together with the evolution of the relative contribution of the non-stationarities per frequency decade over time.

In order to study the impact of the 'stabilization' time on the results of the respective electrochemical techniques in practice, two characteristic times have been selected: one well before the stabilization time and one well after the stabilization time for each respective system. Taking into account the discrete times in which a PP experiment was performed, 1.5 h and 24 h were selected. It needs to be noted that in the case of the LPR technique, where a measurement was performed at discrete times every hour, a LPR value after 1.5 h is obtained from the average of the R_p values after 1 h and 2 h, respectively. In the case of the EN technique, where measurements with a duration of 1 h were performed, the EN values after 1.5 h are taken from the R_n values from the measurements that started after 1 h of immersion and the EN values after 24 h are taken from the measurements starting after 23 h and ending after 24 h. It has been previously discussed that these R_n values are selected because of their equivalence to the polarization resistance [38]. In Fig. 9, the R_ps obtained from LPR, EIS and EN measurements after 1.5 h and 24 h are presented with the related absolute errors on the resistance values. Tables 4 and 5 present an overview of the respective values and their absolute errors after 1.5 h and 24 h, respectively.

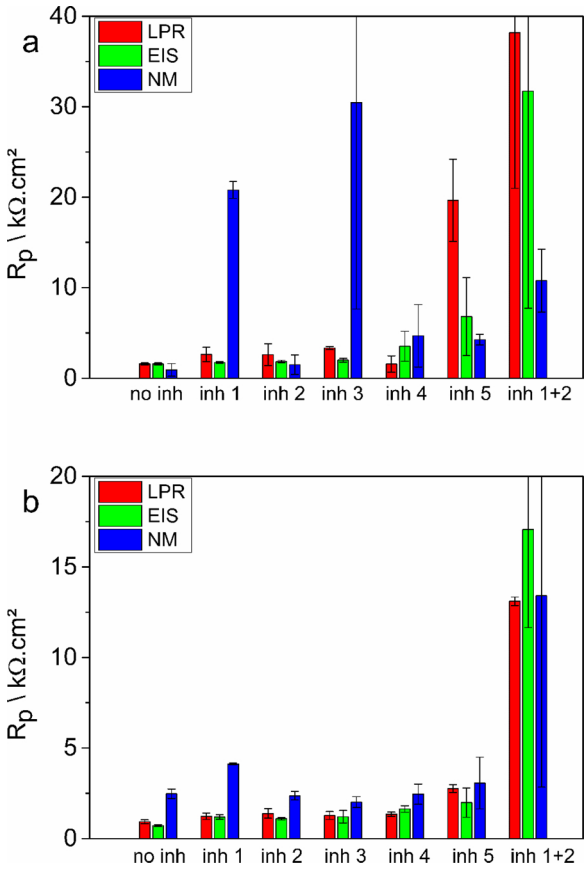

Fig. 9. Overview of the results obtained through linear polarization resistance (LPR), electrochemical impedance spectroscopy (EIS) and electrochemical noise (EN) measurements for hot-dip galvanized steel with and without corrosion inhibitor after 1.5 h **(a)** and **(b)** 24 h. Inhibitor 1 (Novinox®ACE110); inhibitor 2 (Novinox®XCA02); inhibitor 3 (Halox®SW-111); inhibitor 4 (Heucophos® CAPP); inhibitor 5 (Zinc Phosphate ZP10).

Table 4
R_p values with their absolute error obtained from LPR and EIS measurements and R_n values obtained from EN measurments after 1.5 h.

	LPR		EIS		EN	
	Value (kΩ.cm²)	abs. error (kΩ.cm²)	Value (kΩ.cm²)	abs. error (kΩ.cm²)	Value (kΩ.cm²)	abs. error (kΩ.cm²)
no inh	1.58	0.12	1.57	0.12	0.92	0.70
inh 1	2.62	0.80	1.74	0.10	20.78	0.93
inh 2	2.60	1.20	1.84	0.14	1.49	1.08
inh 3	3.34	0.17	1.99	0.20	30.47	22.83
inh 4	1.57	0.90	3.53	1.65	4.68	3.44
inh 5	19.65	4.55	6.79	4.30	4.25	0.59
inh 1 + 2	38.19	17.23	31.71	24.00	10.77	3.47

From the results after 1.5 h, it can be seen that the system containing corrosion inhibitor 5 and the system containing corrosion inhibitor 1 + 2 have an increased R_p, compared for the system without corrosion inhibitor and other corrosion inhibitor containing systems. Nevertheless, all corrosion inhibitor containing systems have an increased R_p compared to the system without corrosion inhibitor. After 24 h, however, only the system containing the combination of corrosion inhibitor 1 and 2 has a higher R_p. It needs to be remarked that, as mentioned before, when interpreting the results after 1.5 h (Fig. 9a and Table 4), the system without corrosion inhibitors as well as the systems with corrosion inhibitors suffer from non-stationary behaviour. This causes the overall system's instability as observed from ORP-EIS

Table 5
R_p values with their absolute error obtained from LPR and EIS measurements and R_n values obtained from EN measurments after 24 h.

	LPR		EIS		EN	
	Value ($k\Omega.cm^2$)	abs. error ($k\Omega.cm^2$)	value ($k\Omega.cm^2$)	abs. error ($k\Omega.cm^2$)	Value ($k\Omega.cm^2$)	abs. error ($k\Omega.cm^2$)
no inh	0.93	0.11	0.72	0.05	2.47	0.26
inh 1	1.23	0.18	1.19	0.12	4.11	0.06
inh 2	1.39	0.26	1.09	0.07	2.37	0.23
inh 3	1.27	0.22	1.21	0.35	2.01	0.30
inh 4	1.35	0.12	1.63	0.18	2.45	0.56
inh 5	2.76	0.21	1.98	0.81	3.06	1.43
inh 1 + 2	13.10	0.23	17.07	5.43	13.41	10.57

measurements. Consequently, the errors on the R_ps after 1.5 h are significantly high, especially the errors on the EN measurements due to the DWT procedure used for DC drift removal [12]. However, it is also possible that EN measurements show these instabilities by significantly high standard deviations and consequently untrustworthy R_n values. After 24 h, when the system is stable, good agreement between LPR, EIS and EN is observed, with low standard deviations on the R_n values. This indicates that EN measurements could be an indicator of non-stationary behaviour when the respective standard deviations are taken into account.

For both the LPR and EIS technique, respectively, the R_p of the combination of inhibitor 1 and inhibitor 2 is more than 4 times higher than for the sum of the individual corrosion inhibitors (Fig. 9b and Table 5). This signifies that the system containing both inhibitors is a synergistic combination of these inhibitors.

For the results after 24 h (Fig. 9b and Table 5) all systems are behaving time-invariant resulting in more stable R_p values with lower absolute error. Yet again, it can be confirmed here that the R_p values obtained from LPR and EIS measurements are in good agreement for most of the measurements apart from the measurements containing corrosion inhibitor 5 after 1.5 h. Therefore the systems will be evaluated from now on based mainly on the R_p values obtained from LPR and EIS measurements.

In our previous work, it has been observed that there is a correlation between the stability of electrochemical processes, obtained from ORP-EIS, and the stability of the R_p values obtained from LPR and EIS measurements whereas a substantial difference with the results from EN is observed in the first 24 h after immersion [12]. In this paragraph, the same interpretation is done for the systems discussed here serving as the deciding tool for the trustworthiness of the electrochemical values and of the related effectiveness of the respective corrosion inhibitors. In Fig. 10, the R_p values of the hot-dip galvanized steel without corrosion inhibitors and with corrosion inhibitor 3, 4 and 5 (the phosphate- based corrosion inhibitors) obtained through LPR, EIS and EN measurements and coupled to the relative contribution of the non-stationarities of the ORP-EIS measurements for the first 24 h after immersion. In Fig. 11, the same comparison is made similarly for corrosion inhibitor 1, 2 and the combination of 1 and 2 (the silica- based corrosion inhibitors).

For the hot-dip galvanized steel without corrosion inhibitors (Fig. 10a), the R_p values obtained from LPR and EIS follow a similar

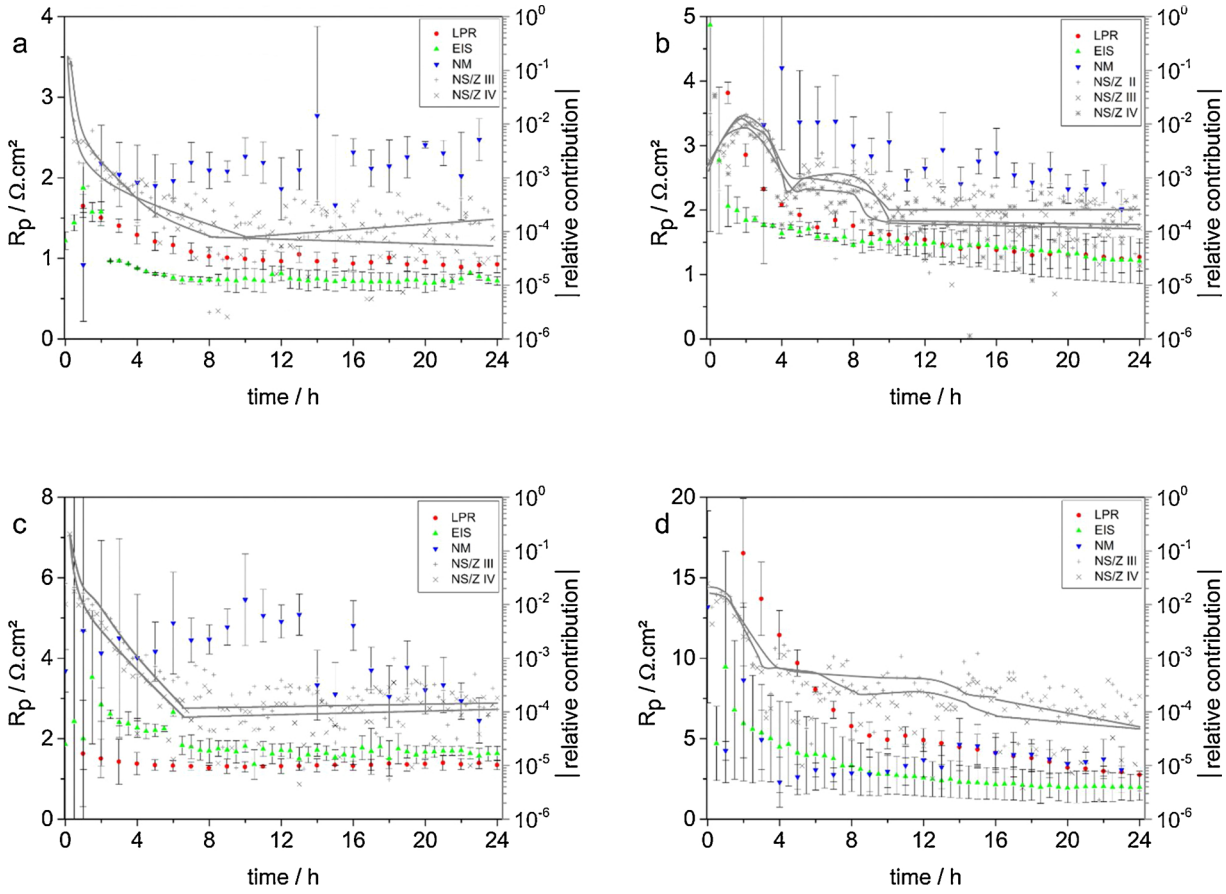

Fig. 10. Overview of the results obtained through linear polarization resistance (LPR), electrochemical impedance spectroscopy (EIS), electrochemical noise (EN) and odd-random-phase electrochemical impedance spectroscopy (ORP-EIS) measurements for hot-dip galvanized steel with and without corrosion inhibitor for 24 h. Without corrosion inhibitors (0.05 mM NaCl) **(a)**, corrosion inhibitor 3 (0.1 mM Halox®SW-111) **(b)**, corrosion inhibitor 4 (0.5 mM Heucophos®CAPP) **(c)** and corrosion inhibitor 5 (0.02 mM Zinc Phosphate ZP10) **(d)**.

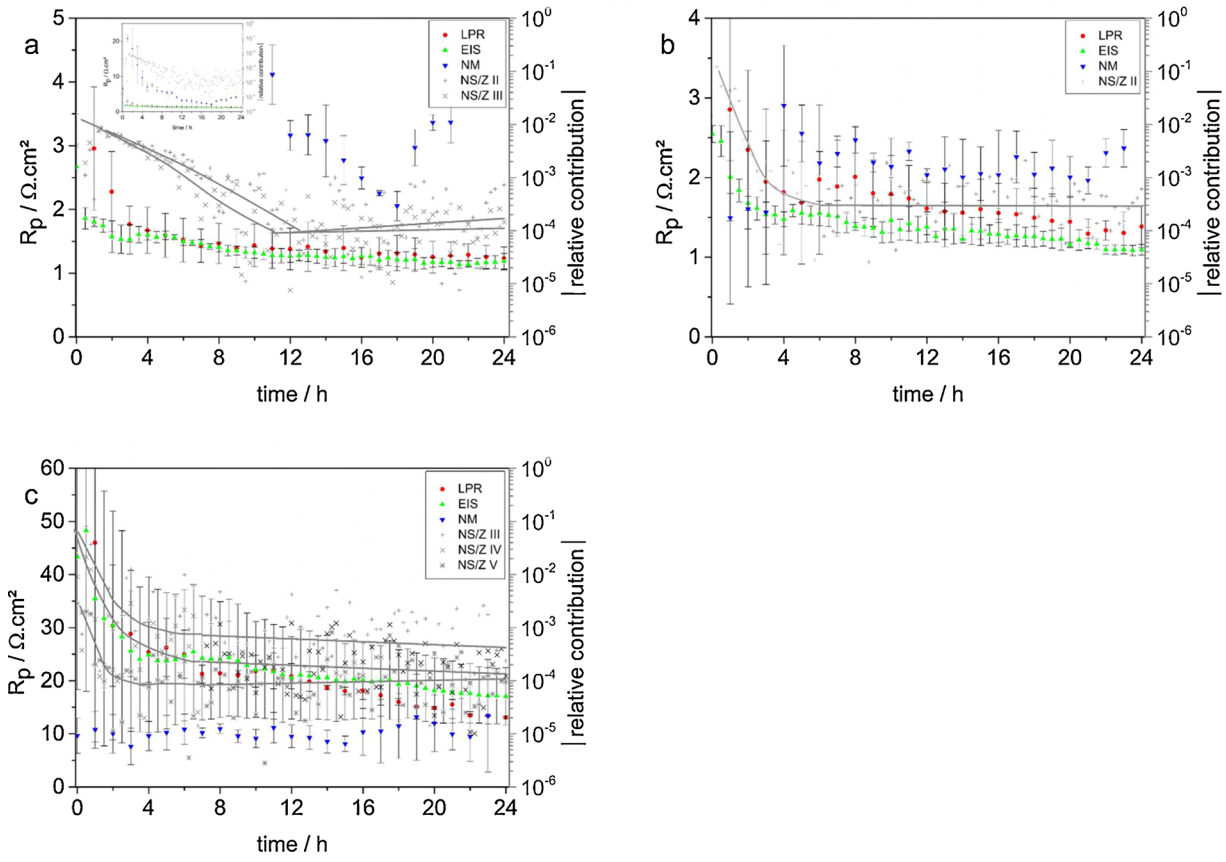

Fig. 11. Overview of the results obtained through linear polarization resistance (LPR), electrochemical impedance spectroscopy (EIS), electrochemical noise (EN) and odd-random-phase electrochemical impedance spectroscopy (ORP-EIS) measurements for hot-dip galvanized steel with corrosion inhibitor 1 (0.5 mM Novinox®ACE110) **(a)**, corrosion inhibitor 2 (0.5 mM Novinox®XCA02) **(b)** and corrosion inhibitor 1 + 2 (both 0.5 mM) **(c)** for 24 h.

trend over the course of the measurement: both decrease strongly in the first 10 h, before reaching a stable value for the rest of the measurement. This time window corresponds to the time the relative contribution of the non-stationarities in frequency decades IV and III needs to become stable. Since these frequency decades were the last to stabilize, as discussed during the ORP-EIS interpretation, these present a fully time-invariant and consequently 'stable' electrochemical system from this point on.

In the case of the hot-dip galvanized steel with corrosion inhibitor 3 (Fig. 10b), three distinct regions in time are observed. In the first hours after immersion, the R_ps obtained through LPR and EIS measurements are substantially different and decrease strongly in the first 4 h. At the same time, the relative contribution of the non-stationarities in frequency decades IV, III and II decreases strongly and stabilizes after 4 h. In the following hours, their contribution remains initially at the same level, before decreasing towards a stable value after 10 h. This is reflected in fluctuations in the R_p values from LPR mainly and stabilization of the R_p obtained from LPR and EIS after 10 h. After 10 h, the system is fully stationary, reflected in stable values of the respective R_p values.

The system containing corrosion inhibitor 4 (Fig. 10c) initially behaves non-stationary, reflected in the high relative contribution of the non-stationarities in the middle frequency region (decades IV and III). This is translated in unstable R_p values obtained from LPR and EIS initially. Afterwards, the relative contribution of the non-stationarities in the middle frequency region decreases towards a stable value after 6.5 h of immersion. At the same time, the R_p values from LPR and EIS decrease gradually in the first 6.5 h. Afterwards, when the system is behaving fully stationary, due to the stabilization of the electrochemical processes with characteristic time-constants corresponding to the mid frequency region, stable values of R_p from both techniques are obtained.

For the hot-dip galvanized steel with corrosion inhibitor 5 (Fig. 10d), the R_p values obtained from LPR and EIS decrease gradually as a function of time towards 16 h of immersion. This time corresponds to the time needed to stabilize, over different plateaus, the electrochemical processes with time-constants corresponding to the middle frequency decades (IV and III). Afterwards, the R_p value obtained from EIS remains stable for the remaining course of the measurement. The R_p value obtained from LPR decreases slightly, but compared to its initial evolution, this slight decrease is negligible.

For the system containing corrosion inhibitor 1 (Fig. 11a), it can be seen that the relative contribution of the non-stationarities in the middle frequency decades (III and II) dominates the instability of the system. Only after 11 and 12 h, respectively, their contribution becomes stable and the system can be considered as time-invariant. This is reflected in the behaviour of the R_p values from LPR and EIS.

For the system containing corrosion inhibitor 2 (Fig. 11b), the 'instability' of the overall electrochemical system is governed by the electrochemical processes with time-constants corresponding to the lower frequency region (decade II) since the relative contribution of the non-stationarities in this frequency decade stabilizes later compared to the middle and higher frequency region. In this case, this is only reflected in the behaviour of the R_p obtained from EIS measurements, which stabilizes after 6 h of immersion and not in the behaviour of the R_p from LPR measurements, which fluctuates at later stages over the course of the measurement.

The R_p of the hot-dip galvanized steel with the combination of

corrosion inhibitor 1 and 2 obtained from LPR and EIS measurements (Fig. 11c) decreases rapidly in the first 3 h after immersion and more gradually towards 7 h after immersion. Afterwards both values tend to stabilize and decrease only slightly over the course of the measurement. A similar trend is observed in the relative contribution of the non-stationarities in the middle (IV and III) and higher frequency (V) decades which stabilize after 7 h respectively.

It can be concluded that it is difficult to compare the electrochemical results obtained with different electrochemical techniques after 1.5 h since the system without corrosion inhibitors as well as the systems with corrosion inhibitors is behaving non-stationary. This is reflected in significantly high errors on the respective R_p values at this stage. After 24 h, when the systems are behaving fully time-invariant, the errors on R_p become smaller. The combination of both inhibitor 1 and 2 is definitely a synergistic combination, based on the comparison between the R_p values from LPR and EIS on the one hand and the values of the individual components on the other hand. In general, before the characteristic stabilization of each respective electrochemical system, when the system is behaving in a non-stationary way, non-stable R_p values from LPR and EIS are obtained. After the characteristic stabilization time, the system behaves in a fully stationary way and stable R_p values from LPR and EIS are obtained for the remaining of the experiment.

4. Conclusions

In this work, different macroscopic electrochemical techniques were applied for the screening of silica- and phosphate- based corrosion inhibitors and corrosion inhibitor synergy for the protection of hot-dip galvanized steel, taking into account the electrochemical time-domain studied by ORP-EIS, leading to the following conclusions:

- The quantitative interpretation per frequency decade of ORP-EIS data indicated that for the phosphate- as well as the silica-based corrosion inhibitors, the non-stationarities are dominating the system's 'instability'. Some corrosion inhibitors effectively stabilize the electrochemical interface while other prolong the electrochemical stability. Nevertheless, the combination of both silica-based corrosion inhibitors stabilizes the electrochemical interface to the largest extent. This effect has an unneglectable impact on the interpretation of the electrochemical results. Initially, the polarization resistance (R_p) or noise resistance (R_n) values obtained from potentiodynamic polarization (PP), linear polarization resistance (LPR), electrochemical impedance spectroscopy (EIS) and electrochemical noise (EN) measurements are generally 'unstable' and suffer from relatively high absolute error. This is due to either the application of a stationary technique in the non-stationary regime or the influence of the non-stationary behaviour on the data treatment procedure. After the period of stabilization, the values are more stable with lower absolute error.
- PP measurements revealed that all corrosion inhibitors are behaving as cathodic corrosion inhibitors, effectively reducing the cathodic current densities.
- LPR measurements revealed that both the phosphate- and silica-based corrosion inhibitors provide immediate corrosion protection as well as protection over the course of the measurement, indicated by an elevated polarization resistance with a factor 2–3 for the inhibitor containing systems and up to 15 for the synergistic combination of both silica-based corrosion inhibitors after 168 h.
- EIS measurements revealed the presence of corrosion inhibitor protective action in the middle frequency region, having a positive effect on the overall performance of the corrosion inhibitor-containing electrochemical systems, indicated by an increased polarization resistance with values comparable to the LPR measurements.
- EN measurements on the phosphate-based corrosion inhibitors revealed no effective corrosion protection over the course of 24 h compared to the system without corrosion inhibitors. For the silica-based corrosion inhibitors, the synergistic action is yet again confirmed.

The results obtained from these macroscopic electrochemical techniques highlight the importance of the electrochemistry in the time-domain and the necessity of detailed (macroscopic) electrochemical analysis.

CRediT authorship contribution statement

M. Meeusen: Conceptualization, Methodology, Validation, Investigation, Writing - original draft. **L. Zardet:** Validation, Investigation. **A.M. Homborg:** Conceptualization, Software. **M. Lekka:** Supervision. **F. Andreatta:** Validation, Investigation. **L. Fedrizzi:** Supervision. **B. Boelen:** Resources. **J.M.C Mol:** Conceptualization, Methodology, Supervision. **H. Terryn:** Conceptualization, Methodology, Supervision.

Declaration of Competing Interest

The authors declare that they have no known competing financial interests or personal relationships that could have appeared to influence the work reported in this paper.

Acknowledgements

This research was carried out under project number F81.6.13503 in the framework of the Partnership Program of the Materials innovation institute M2i (www.m2i.nl) and the Foundation for Fundamental Research on Matter (FOM), which is part of the Netherlands Organization for Scientific Research NWO (www.nwo.nl).

Ruud Hendrikx at the Department of Materials Science and Engineering of the Delft University of Technology is acknowledged for the X-ray analysis.

Appendix A. Supplementary data

Supplementary material related to this article can be found, in the online version, at doi:https://doi.org/10.1016/j.corsci.2020.108780.

References

[1] O. Gharbi, S. Thomas, C. Smith, N. Birbilis, Chromate replacement: what does the future hold? Npj Mater. Degrad. 2 (1) (2018) 12.
[2] S.A. Umoren, M.M. Solomon, Synergistic corrosion inhibition effect of metal cations and mixtures of organic compounds: a review, J. Environ. Chem. Eng. 5 (1) (2016) 246–273.
[3] S.R. Taylor, B.D. Chambers, Identification and characterization of nonchromate corrosion inhibitor synergies using high-throughput methods, Corrosion 64 (3) (2008) 255–270.
[4] C. Feiler, D. Mei, B. Vaghefinazari, T. Wurger, R.H. Meissner, B.J.C. Luthringer-Feyerabend, D.A. Winkler, M.L. Zheludkevich, S.V. Lamaka, In silico screening of modulators of magnesium dissolution, Corros. Sci. 163 (2019) 108245.
[5] M. Ebrahimi, T. Shahrabi, M.G. Hosseini, Determination of suitable corrosion inhibitor formulation for a potable water supply, Anti-corrosion Methods Mater. 51 (6) (2004) 399–405.
[6] R. Romagnoli, M.C. Deyá, B. Del Amo, The mechanism of the anticorrosive action of calcium-exchanged silica, Surf. Coat. Int. Part B Coat. Trans. 86 (2) (2003) 135–141.
[7] N. Granizo, M.I. Martín, F.A. López, J.M. Vega, D. De La Fuente, M. Morcillo, Chemical and structural changes of calcium ion exchange silica pigment in 0.5M NaCl and 0.5M Na_2SO_4 solutions, Afinidad 68 (556) (2011) 439–446.
[8] R. Naderi, S.Y. Arman, S. Fouladvand, Investigation on the inhibition synergism of new generations of phosphate-based anticorrosion pigments, Dye. Pigment. 105 (2014) 23–33.
[9] M. Mahdavian, M.M. Attar, Evaluation of zinc phosphate and zinc chromate effectiveness via AC and DC methods, Prog. Org. Coat. (2005) 191–194.
[10] F. Askari, E. Ghasemi, B. Ramezanzadeh, M. Mahdavian, Synthesis and characterization of the fourth generation of zinc phosphate pigment in the presence of benzotriazole, Dye. Pigment. 124 (2016) 18–26.
[11] M. Bethencourt, F.J. Botana, M. Marcos, R.M. Osuna, J.M. Sánchez-amaya,).

Inhibitor properties of “green” pigments for paints, Prog. Org. Coat. 46 (2003) 280–287.
[12] M. Meeusen, L. Zardet, A.M. Homborg, M. Lekka, B. Boelen, H. Terryn, et al., Complementary electrochemical approach for time-resolved evaluation of corrosion inhibitor performance, J. Electrochem. Soc. 166 (11) (2019) 3220–3232.
[13] A.S.T.M.D. 6386, Standard Practice for Preparation of Zinc (Hot-Dip Galvanized) Coated Iron and Steel Product and Hardware Surfaces for Painting, Annual Book of ASTM Standards, 2005.
[14] Y. Van Ingelgem, E. Tourwé, O. Blajiev, R. Pintelon, A. Hubin, Advantages of odd random phase multisine electrochemical impedance measurements, Electroanalysis 21 (6) (2009) 730–739.
[15] E. Van Gheem, R. Pintelon, J. Vereecken, J. Schoukens, A. Hubin, P. Verboven, O. Blajiev, Electrochemical impedance spectroscopy in the presence of non-linear distortions and non-stationary behaviour Part I: Theory and validation, Electrochim. Acta 49 (26) (2004) 4753–4762.
[16] K.E. Atkinson, J. Wiley, An Introduction to Numerical Analysis, second edition, (1978).
[17] T.J. Cole, Too many digits: the presentation of numerical data, Arch. Dis. Child. 100 (7) (1984) 608–609.
[18] R. Kordi, Sports medicine update, Scand. J. Med. Sci. Sports 21 (2011) 867–868.
[19] ASTM, ASTM G3-89 Standard Practice for Conventions Applicable to Electrochemical Measurements in Corrosion Testing, 89(Reapproved), 1–10 (1999).
[20] F. Mansfeld, Fundamental aspects of the polarization resistance technique-the early days, J. Solid State Electrochem. 13 (4) (2009) 515–520.
[21] A.M. Homborg, E.P.M. Van Westing, T. Tinga, G.M. Ferrari, X. Zhang, J.H.W. De Wit, J.M.C. Mol, Application of transient analysis using Hilbert spectra of electrochemical noise to the identification of corrosion inhibition, Electrochim. Acta 116 (2014) 355–365.
[22] A.M. Homborg, T. Tinga, X. Zhang, E.P.M. Van Westing, P.J. Oonincx, J.H.W. De Wit, J.M.C. Mol, Time-frequency methods for trend removal in electrochemical noise data, Electrochim. Acta 70 (2012) 199–209.
[23] A.M. Homborg, R.A. Cottis, J.M.C. Mol, An integrated approach in the time, frequency and time-frequency domain for the identification of corrosion using electrochemical noise, Electrochim. Acta 222 (2016) 627–640.
[24] I.A. Kartsonakis, S.G. Stanciu, A.A. Matei, R. Hristu, A. Karantonis, C.A. Charitidis, A comparative study of corrosion inhibitors on hot-dip galvanized steel, Corros. Sci. 112 (2016) 289–307.
[25] M. Mouanga, P. Berçot, Comparison of corrosion behaviour of zinc in NaCl and in NaOH solutions; Part II: Electrochemical analyses, Corros. Sci. 52 (12) (2010) 3993–4000.
[26] V. Barranco, S. Feliu, S. Feliu,). EIS study of the corrosion behaviour of zinc-based coatings on steel in quiescent 3% NaCl solution. Part 1: Directly exposed coatings, Corros. Sci. 46 (9) (2004) 2203–2220.
[27] C. Deslouis, M. Duprat, C. Tournillon, The kinetics of zinc dissolution in aerated sodium sulphate solutions. A measurement of the corrosion rate by impedance techniques, Corros. Sci. 29 (1) (1989) 13–30.
[28] P.S.G. Da Silva, A.N.C. Costa, O.R. Mattos, A.N. Correia, P. De Lima-Neto, Evaluation of the corrosion behavior of galvannealed steel in chloride aqueous solution and in tropical marine environment, J. Appl. Electrochem. 36 (3) (2006) 375–383.
[29] E.P.M. van Westing, G.M. Ferrari, J.H.W. de Wit, The determination of coating performance with impedance measurements-IV. Protective mechanisms of anticorrosion pigments, Corros. Sci. 36 (8) (1994) 1323–1346.
[30] M.L. Zheludkevich, K.A. Yasakau, A.C. Bastos, O.V. Karavai, M.G.S. Ferreira, On the application of electrochemical impedance spectroscopy to study the self-healing properties of protective coatings, Electrochem. commun. 9 (10) (2007) 2622–2628.
[31] R.A. Buchanan, E.E. Stansbury, Handbook of Environmental Degradation of Materials, (2012).
[32] K.M. Ismail, Evaluation of cysteine as environmentally friendly corrosion inhibitor for copper in neutral and acidic chloride solutions, Electrochim. Acta 52 (28) (2007) 7811–7819.
[33] G.E. Badea, A. Caraban, M. Sebesan, P. Cret, A. Setel, Polarisation Measurements Used for Corrosion Rates Determination, Journal of Sustenable Energy 1 (1) (2010) 1–4.
[34] J.R. Macdonald, E. Barsoukov, Impedance Spectroscopy Theory, Experiment, and Applications Vol. 125 Wiley intersience, 2005 Wiley-Interscience.
[35] D.D. Macdonald, M. Urquidi-Macdonald, Application of Kramers - Kronig Transforms in the Analysis of Electrochemical Systems, Soc, J Electrochem 123 (1985) 2316.
[36] B.N. Popov, Corrosion Engineering Principles and Solved Problems - Corrosion of Structural Concrete, (2015).
[37] Z. Dong, X. Guo, J. Zheng, L. Xu, Calculation of noise resistance by use of the discrete wavelets transform, Electrochem. commun. 3 (10) (2001) 561–565.
[38] J.F. Chen, W.F. Bogaerts, The Physical meaning of noise resistance, Corros. Sci. 37 (11) (1995) 1839–1842.